GREEN SYNTHESIS OF PANI/MAGNETITE ADSORBENT USING *CROTON MACROSTACHYUS* LEAF EXTRACT FOR REMOVAL OF RHODAMINE BLUE DYE FROM AQUEOUS SOLUTION.

A THESIS SUBMITTED TO DEPARTMENT OF CHEMISTRY IN PARTIAL FULFILMENT OF THEREQUIREMENTS FOR MASTERS OF SCIENCE IN APPLIED CHEMISTRY COLLEGE OF NATURAL AND COMPUTATIONAL SCIENCE

POSTGRADUATE STUDIES WOLKITE UNIVERSITY

BY:

YESHIWAS DAGNAW YEWALA

January, 2025 G.C.

Wolkite, Ethiopia

Green Synthesis of PANI/Magnetite AdsorbentUsing *Croton Macrostachyus* L eaf Extract for Removal of Rhodamine Blue Dye from Aqueous Solution.

Yeshiwas Dagnaw Yewala

Advisor; - Dr. Israel Leka (PhD)

Co-advisor: Teshale Assefa (PhD)

A Thesis Submitted to Department of Chemistry,

College of Natural and Computational Sciences

Wolkite University

January, 2025 G.C.

Wolkite, Ethiopia

RECOMMENDATION

As the primary advisor for this study, I attest that I read the draft thesis, "Green synthesis of PANI/magnetite adsorbent using croton *macrostachyu*s leaf extract for removal of rhodamine blue dye from aqueous solution," and that I provided the student with close guidance throughout its development. Prepared with Yeshiwas Dagnaw's assistance. As a result, I advise sending the study to the department for additional assessment and review.

Major advisor

Israel Leka (PhD) Signature_____ Date_____

APPROVAL SHEET

I, the advisor of the thesis entitled "**Green synthesis of PANI/magnetiteadsorbent using *croto n macrostachyus* leaf extract for removal of rhodamine blue dye from aqueous solution"** an d developed by Yeshiwas Dagnaw, hereby certify that the recommendation and suggestions made by the board of examiners are appropriately incorporated into the final version of the thesis.

Major advisor

Israel Leka (PhD) Signature _____ date _____

Co- advisor

Teshale Assefa (PhD) Signature _____ date _____

EXAMINER'S APPROVAL SHEET

We, the undersigned, members of the Board of Examiners of the thesis by Yeshiwas Dagnaw have read and evaluated the thesis entitled "**Green synthesis of PANI/magnetite adsorbent using *croton macrostachyus* leaf extract for removal of rhodamine blue dye from aqueous s olution"** and examined the candidate during the open defense. Therefore, to certify that the thesi s is accepted for partial fulfillment of the requirement of the degree of Master of Science in Chemistry.

Chairperson

Ermias Tamiru (PhD) Signature _____ Date _____

Internal Examiner

NigussieAlebachew (PhD) Signature _____ Date _____

External Examiner

Fedilu Kedir (PhD) Signature _____ Date_____

Final approval and acceptance of the thesis are contingent upon the submission of its final copy to the Office of Postgraduate Studies (OPGS) through the Department Graduate Council (DGC) and School Graduate Committee (SGC).

NigussieAlebachew (PhD) Signature_____ Date_____

Department Head

_____ _____ _____

College of post graduate coordinator Signature Date

_____ _____ _____

Name of school of graduate Studies, Dean Signature Date

DECLARATION

This thesis, "Green synthesis of PANI/magnetite adsorbent using *croton macrostachyus* leaf extract for removal of rhodamine blue dye from aqueous solution," is my unique work, therefore declare. In other words, it hasn't been submitted to another university for the award of any academic degree, diploma, or certificate. Each and every source of information used in this thesis has been properly cited.

Yeshiwas Dagnaw Signature_____ Date_____

Name of Student

ABSTRACT

In this study, a green synthesis approach was employed to create adsorbent consisting of polyaniline (PANI) and magnetite (Fe_3O_4) nanoparticles using an aqueous extract of Croton macrostachyus *leaves. To characterize the structural, chemical, and optical properties of the synthesized materials, several analytical techniques were employed. The XRD results indicated that the average particle size of the PANI/Fe_3O_4 adsorbent was approximately 14 nm, suggesting that the material consisted of nanoscale particles, which is crucial for improving the surface area and reactivity of the adsorbent. UV-DRS analysis revealed that the nanocomposite exhibited broad absorbance peaks between 700 and 800 nm. FTIR spectroscopy confirmed the presence of functional groups corresponding to PANI/Fe_3O_4, PANI and Fe_3O_4, and the phytochemicals in the* Croton macrostachyus *leaf extract. The adsorptive efficiency of each material was evaluated under varying experimental conditions, such as pH, adsorbent dose, contact time, and initial dye concentration. The results showed that the optimum conditions for dye removal occurred at a pH of 10, an adsorbent dose of 80 mg, a contact time of 50 minutes, and an initial dye concentration of 10 mg/L. Under these conditions, the dye removal efficiencies were 91.22% for PANI, 96.97% for Fe_3O_4, and 99.91% for the PANI/Fe_3O_4 adsorbent, demonstrating exhibited superior dye removal performance. To further understand the adsorption behavior, adsorption isotherm models were applied. The results indicated that the adsorption of Rhodamine Blue dye onto all three adsorbents (PANI, Fe_3O_4, and the nanocomposite) was best described by the Langmuir isotherm, suggesting that the adsorption occurred via a monolayer adsorption process with uniform adsorption sites. In contrast, the Freundlich isotherm, which models heterogeneous adsorption, did not fit as well, indicating that the adsorption sites on the materials were relatively uniform. Additionally, the adsorption kinetics were found to follow the pseudo-second-order model, suggesting that the rate-limiting step of the dye removal process was chemical adsorption. The findings from this study underscore the potential of the green-synthesized PANI/Fe_3O_4 adsorbent as a highly effective and environmentally friendly adsorbent for the removal of organic dyes from wastewater.*

***Keywords**: Nanocomposite, adsorbent, Rhodamine blue, Croton macrostachyus, green synthesis*

ACKNOWLEDGEMENT

First and foremost, I would like to thank the Almighty God and his mother, St. Mary, for giving me the health, strength, wisdom, and patience to complete this thesis.

Second, I would like to express my deepest gratitude and thanks to my advisor, Dr. Israel Leka (PhD), for his cooperation, suggestions, supervision, and remarks; appreciable encouragement; fatherly consultation; and taking his time to read and correct my document, starting from the proposal writing to the completion of this thesis.

I would like to thank my co-advisor, Teshale Assefa (PhD), for his cooperation, suggestions, supervision, and remarks; appreciable encouragement; and taking his time to read and correct my document, starting from the proposal writing to the completion of this thesis.

I would like to thank my family for continuous financial and moral support.

I would like to thank College of natural and computational science, Inorganic Chemistry Technician (Mr. Alemayehu Worku), Chemistry Department, and all individuals who supported me by sharing ideas or offering materials support which is an input for this work.

I would like to thank the Ministry of Education for giving the MSc learning program.

I would like to thank Wolkite University Chemistry Department for UV-vis analysis in the adsorption experiment.

I would like to thank Addis Ababa Sciences and Technology University, Central Laboratory, for FT-IR, XRD analysis

TABLE OF CONTENTS

LIST OF FIGURES

LIST OF TABLE

LIST OF ABBREVIATIONS

APS	Ammonium per sulfate
FTIR	Fourier transform infrared spectroscopy
MNP	Magnetic nanoparticles
NCs	Nan composites
pHpzc	pH of point zero charge
PANI	Polyaniline
RB	Rhodamine blue
XRD	X-ray diffraction
DRS	Diffuse reflectance spectroscopy
NPs	Nanoparticles

CHAPTER ONE
INTRODUCTION

1.1 Background of the study

The management of water resources is indeed one of the most pressing challenges facing both local and global communities today. The water cycle, which governs the distribution, movement, and availability of water, plays a crucial role in sustaining both human populations and natural ecosystems. However, human activities—particularly in industrial and agricultural sectors—have significantly disrupted the delicate balance of this cycle, leading to concerns over the availability and quality of freshwater resources [1]. Water supply pollution by pollutants, such as heavy metals, synthetic dyes, and hazardous compounds, has grown to be a global environmental concern. In addition to endangering water's portability, these pollutants also impair aquatic ecosystems' ecological health, decreasing biodiversity and destroying many species' habitats. When released into water systems, dyes—which are widely used in industries including textiles, pulp and paper manufacture, carpet manufacturing, and leather tanning—are known to have detrimental effects on the environment. IN many different production processes, dyes—which are frequently composed of intricate chemical compounds—are usually utilized in enormous quantities. They present major health and environmental hazards when released into water bodies without being properly treated. Colorants found in these industrial effluents are frequently tenacious and challenging to break down, contaminating groundwater supplies, lakes, and rivers.

Numerous synthetic dyes are particularly harmful because they can cause cancer, mutagenesis, or teratogenicity in both people and animals. As soon as these dyes get into the water cycle, they can interfere with the oxygen transfer, light penetration, and nutrient cycling processes that are vital to the wellbeing of aquatic ecosystems. Additionally, the hue of contaminated water detracts from its aesthetic attractiveness, making it less suitable for recreational and human consumption. Water contaminated with dyes has serious negative effects on health. People who are exposed to dye-contaminated water may have a variety of acute and long-term health problems, such as headaches, nausea, vomiting, and skin irritation. More serious consequences can include bone marrow suppression, which can result in diseases like anemia, and harm to internal organs like the liver and kidneys [2].Dyes in water can also lead to waterborne illnesses, which are spread by drinking or coming into touch with tainted water. Diarrhea, mucous membrane and skin ulcers,

and severe dermatitis are some of the symptoms that these conditions might produce. These public health problems put a heavy strain on healthcare systems, especially in developing nations with limited access to sanitary facilities and clean water. It is imperative to put into practice efficient water treatment techniques because dye contaminants are pervasive and have a negative impact on the environment and human health Methods such as adsorption, filtration, and biological treatments have been explored to remove or neutralize dyes in wastewater. Among these, the development of green or eco-friendly materials for dye removal, such as nanocomposites made from natural polymers and nanoparticles, presents a promising solution. These materials not only exhibit high adsorption capacity but are also sustainable, minimizing the environmental impact compared to traditional chemical treatments. For example, materials like polyaniline (PANI) combined with magnetite nanoparticles (Fe_3O_4), synthesized using plant extracts such as Croton macrostachyus, have shown significant potential in adsorbing toxic dyes like Rhoda mine Blue (RhB) from aqueous solutions. This innovative approach could play a key role in addressing the global challenge of water pollution, ensuring cleaner water resources for future generations.

Several techniques, such as flotation, chemical coagulation, chemical oxidation, and adsorption, are commonly employed to eliminate color from wastewater [3-5]. Among these, adsorption stands out as a promising method for wastewater treatment due to its low cost, ease of implementation, and ability to perform cleaning without generating sludge. For many years, activated carbon has been the preferred adsorbent for dye removal due to its high surface area and effectiveness. However, activated carbon remains relatively expensive, prompting ongoing research into more affordable alternative adsorbents. Recent studies have explored the use of metal oxide nanoparticles, clays, metal hydroxides, and agricultural wastes (such as bagasse pith and sunflower stalks) as low-cost adsorbents for dye removal from wastewater and other aqueous solutions [6 - 8].In recent years, iron-based nanoparticles have gained widespread attention for their application in environmental remediation as adsorbents. These nanoparticles, especially magnetite (Fe_3O_4), possess strong magnetic properties, allowing for easy separation of the adsorbent from theadsorb ate using a simple magnet. Magnetite, a naturally occurring iron oxide, exhibits the highest magnetism among all naturally available minerals, making it a promising candidate for water treatment. While bare magnetite nanoparticles (MNP) have been shown to effectively remove toxic contaminants from water, challenges such as auto-oxidation, agglomeration, and concerns over their toxicity in real-life applications remain significant. Recent studies have addressed these

challenges by depositing or coating natural organic matter on the surface of MNPs, which helps to reduce their toxicity and prevent agglomeration and oxidation, making them more environmentally friendly [9].Polyaniline (PANI), one of the most important and widely studied conducting polymers, offers unique electrical and photoelectric properties. These properties can be easily modified by oxidizing the PANI chain or protonating the imine nitrogen backbone, which enhances its process ability and environmental stability [10]. PANI is also known for its photo catalytic properties, where it functions as an electron donor in various catalytic and electrical processes. In recent years, PANI-based composites with metal oxide nanoparticles, such as ZnO, CdS, and CuS, have attracted considerable attention due to their potential applications in photo catalysis and electrochemical processes [11]. Among the metal oxide nanoparticles, magnetite (Fe_3O_4) has been particularly promising when combined with PANI to form nanocomposites with superior properties for environmental remediation. The use of Croton macrostachyus leaves for the green synthesis of PANI/Fe_3O_4 nanocomposites offers several advantages, including resource recycling, cost reduction, and minimal environmental impact. The aqueous extract of Croton macrostachyus serves as both a reducing and capping agent in the synthesis process, which helps stabilize the nanoparticles and prevent their agglomeration. Additionally, the plant extract contains natural chemicals that assist in the formation of nanoparticles without the need for hazardous chemicals typically used in traditional nanoparticle synthesis. This green synthesis approach aligns with the growing demand for environmentally friendly and sustainable methods of nanoparticle production [12-14]. The potential for using Croton macrostachyus leaf extracts to synthesize PANI/Fe_3O_4 nanocomposites not only offers a more eco-conscious alternative to conventional methods but also contributes to resource efficiency and cost reduction. While the use of PANI/Fe_3O_4 nanocomposites for dye removal has been well-documented, research specifically focusing on the adsorption of Rhodamine Blue (RhB) dye onto the surface of PANI/Fe_3O_4 composites is still lacking. This study aims to bridge that gap by exploring the green synthesis of PANI/Fe_3O_4 nanocomposites through in situ polymerization of PANI with Fe_3O_4 nanoparticles, using ammonium per sulfate (APS) as an initiator. The resulting nanocomposites demonstrate a synergistic effect between PANI and Fe_3O_4 nanoparticles, making them highly effective adsorbents for the removal of RhB dye from aqueous solutions. This research offers valuable insights into the potential applications of PANI/Fe_3O_4 nanocomposites as a sustainable and efficient solution for dye removal in water treatment processes.

1.2 Statement of the problem

Pollution, particularly water contamination, remains a significant global issue. Numerous industries, including textile, paper, plastic, leather, liquid crystal displays (LCDs), solar cells, food production, and mineral processing, extensively use dyes and pigments. These industries generate effluents containing harmful dyes and pigments, which, when released into the environment, cause considerable ecological and human health concerns. Effluents from factories such as those in carpet manufacturing, dyeing, pulp and paper production, and textiles rapidly deteriorate the quality of receiving water sources.

Human exposure to these contaminated waters can lead to various health issues, including skin rashes, nausea, severe headaches, diarrhea, and other waterborne diseases such as anemia, kidney damage, dermatitis, ulceration of the ski.

Recently, natural bentonite and iron-pillared bentonite have emerged as promising low-cost adsorbents for dye removal. Therefor this research focuses on the synthesis of a cost-effective, environmentally friendly bio sorbent using *Croton macrostachyus* leaf extract—an approach not previously explored for the synthesis of polyaniline (PANI) and magnetite nanoparticles (Fe_3O_4) adsorbent.

The primary goal is to develop a sustainable adsorbent capable of efficiently removing Rhodamine Blue (RhB) dye from wastewater or aqueous solutions. This innovative composite has the potential to address the growing need for effective, affordable water treatment solutions.

1.3 Objectives

1.3.1 General objective

The general objective of this study were to synthesize the PANI/magnetite adsorbent using *Croton macrostachyus* leaf extract by polymerization method and applying the nanocomposite for removal of rhodamine blue dye from aqueous solution.

1.3.2 Specific objectives

- To synthesize PANI/Fe_3O_4 adsorbent using leaf extract of *Croton macrostachyus*
- To characterize PANI/Fe_3O_4 adsorbent using leaf extract of *Croton macrostachyus*
- To evaluate the effect of adsorption parameters towards the rhodamine blue dye removal performance of PANI/Fe_3O_4 adsorbent
- To study the adsorption isotherm and kinetics models of PANI/ adsorbent

1.4 Significance of the study

This study offers valuable insights into the green synthesis of PANI/magnetite (Fe_3O_4) adsorbent *using Croton macrostachyus* leaf extract through a polymerization method.

This study is an important contribution to the growing body of research on green nanotechnology, as it demonstrates the potential for plant-based materials to play a significant role in the production of functional nanocomposites for environmental applications. By employing *Croton macrostachyus* leaf extract, the study provides a new avenue for the development of bio-synthesized composites that could be explored in future investigations. Another significant contribution of this study is that it presents a simple, efficient, and cost-effective method for separating the synthesized PANI/Fe_3O_4 adsorbent from the solution. Moreover, this study provides valuable guidance to the scientific community and industry stakeholders on the use of bio-synthesized PANI/magnetite as effective adsorbents for dye removal.

The research highlights how this adsorbent material, synthesized using a natural extract, can be applied in wastewater treatment to remove harmful dyes like Rhodamine Blue (RhB), which is commonly found in industrial effluents. By demonstrating the high adsorption capacity of the PANI/Fe_3O_4 nanocomposite, the study sets a precedent for future research focused on environmentally friendly alternatives to traditional chemical methods for water purification. Additionally, it contributes to the growing trend of using biomaterials in pollution control, paving the way for more sustainable and cost-effective solutions to global water pollution issues.

1.5 Scope of the study

The scope of this study was specifically focused on the synthesis of PANI/magnetite (Fe_3O_4) adsorbent using *Croton macrostachyus* leaf extract through a polymerization method, followed by the characterization of the resulting adsorbent using UV-Vis, XRD, and FTIR spectroscopic techniques. The primary aim was to explore the potential of this bio-synthesized adsorbent material for the removal of Rhodamine Blue (RhB) dye from aqueous solutions.

Key limitations of the study include**:** Scope of Synthesis Method, characterization Techniques: The study relied on a limited number of characterization techniques—UV-Vis spectroscopy, X-ray diffraction (XRD), and Fourier-transform infrared (FTIR) spectroscopy. While additional techniques such as SEM (Scanning Electron Microscopy), TEM (Transmission Electron Microscopy), and BET surface area analysis could provide more detailed information on the morphology, particle size, and surface area of the adsorbent.

Single Dye Focus: The study was limited to investigating the removal of Rhodamine Blue dye (RhB) from aqueous solutions. Although widely studied and toxic dye, testing the nanocomposite's ability to adsorb other dye pollutants or heavy metals from water would provide a more comprehensive understanding of its effectiveness and potential applications in wastewater treatment.

Batch Experimental Setup: The adsorption tests conducted in the study were carried out in batch experiments. While batch studies are valuable for understanding the overall adsorption capacity of the material, continuous flow systems, which more closely simulate real-world conditions, would be necessary to fully assess the practical viability of the PANI/magnetite adsorbent in large-scale applications.

Limited Environmental Conditions: The study primarily focused on the adsorption of RhB dye at specific pH levels (optimized for PANI/Fe_3O_4 adsorbent performance) and under controlled conditions. Further research could explore the effect of various environmental factors—such as temperature, ionic strength, or the presence of competing ions—on the performance of the nanocomposite.

Generally these limitations suggest that further research is needed to enhance the understanding of the material's behavior under a broader range of conditions, explore alternative synthesis methods, and evaluate its performance for diverse pollutants beyond RhB dye

CHAPTER TWO

2 LITERATURE REVIEW

2.1 Water pollution

Water pollution is an important global issue that affects human health, wildlife health, and ecosystem health. Pollutants in water can damage aquatic life, which reduces biodiversity and disturbs fragile ecosystems. Contaminated water sources can cause a variety of health issues, including cancer, respiratory disorders, and gastrointestinal issues [15]. In order to address this problem, it is critical to understand the root causes of water contamination and work toward developing long-term solutions. A significant cause of water pollution is industrial waste. Frequently, factories and other production facilities release dangerous chemicals and pollutants into nearby bodies of water, causing contamination that makes the water unsafe for both people and wildlife [16]. The runoff of pesticides, fertilizers, and animal waste from agriculture greatly contributes to water pollution by contaminating rivers and lakes, resulting in oxygen deprivation and algae blooms [17]. When elements or conditions in water make it unfit for a particular application, the water is considered contaminated. Excessive concentrations of a hazardous substance (pollutants) in water that render it unfit for drinking, cooking, bathing, or other uses are referred to as water pollution. Pollution is the introduction of toxins into the environment. Farming, daily human activities, industrialized and marketable waste, and—above all—carrying mechanisms are all factors in it. In many respects, no matter where you go or what you do, remnants of the earth's environment and its inhabitants are still present. Water contamination and its management in both situations are the main topics of this study [18].Water contamination is defined as the presence of substances or situations that make it unfit for a particular application., according to is defined as the presence of excessive concentrations of a danger (pollutants) in water to the point where it is no longer appropriate for bathing cooking, drinking, or other purposes. The introduction of contaminants into the environment is referred to as pollution. In many ways, the earth's environment and its inhabitants are still present no matter where you go or what you do. The focus of this research is on water pollution and control in both cases. Water is considered polluted if it contains substances or conditions that prevent it from being used for a certain purpose. Other factors that contribute to it include industrialized and marketable garbage, farming activities, everyday human activities, and—most importantly—carrying modes is characterized by the

presence of dangerous (pollutant) concentrations in water that are so high that they are unfit for drinking, cooking, bathing, or other uses. Pollution is the term used to describe the release of pollutants into the environment [18].

2.2 **Dye Chemistry**

Over 3000 synthetic textile colors are currently created and used in a wide range of industrial activities. In addition, the production, dyeing, and printing of dyes include the usage of about 8000 more chemicals. The usage of synthetic dyes has rapidly increased during the last 10 years, particularly in the textile industry. Worldwide, it is estimated that more than 2,105 tons of textile dyes are discharged annually [19].Colored chemicals should not be found in water that is intended for human consumption. Notably, up to 15% of the mass-produced colors may be lost in the effluents during the dyeing process. An estimated 1 million people may be at danger due to severe and protracted water contamination caused by the improper and uncontrolled release of textile effluents into the environment, particularly to surface water habitats. It should be mentioned that the ecological toxicological risk of dyes and colorants is yet mostly unknown [20].

They must be regarded as potentially dangerous for species living in freshwater aquatic habitats because of the substantial amount of colorants that are thought to be lost to waste streams and are not treated by traditional wastewater treatment. According to recent aquatic toxicity research, which focused on 42 commercial synthetic colorants used in textile dyeing, algae may be more susceptible to colorants than Daphnis, especially when the impact of biomass is taken into account. A variety of synthetic dyes, including azo anthraquinonoid, sulfur, indigo, triphenylmethyl, and phthalocyanine derivatives, can be categorized according to their chemical structure and the presence of chromospheres and/or auxochromes groups. Auxochromes may intensify the color of the dye [21]. Also, acidic groups, such as the carboxylic group (COOH) or the sulfonic group (SO3H), are frequently added to the dye structure to make it more soluble in water. As sodium salts, they are typically utilized. Azo dyes are a highly significant class of commercial dyes and adaptable colorants. Especially when compared to natural dyes, these colorants have been overused in industries all over the world because of their large range of color colors, high wet fastness profiles, and ease and affordability of manufacture. The presence of heavy metals like copper, arsenic, lead, cadmium, mercury, nickel, cobalt, and chromium, as well as parent compounds and their breakdown products with reactive groups like sulfur, naphtha, and nitrates and aromatic rings, makes textile effluents extremely toxic. Furthermore, hazardous additional

chemicals used in dyeing processes, such as organic acids, surfactants (such as soaps and hydrocarbon-based softeners), formaldehyde-based dye fixing agents, chlorinated stain removers, and other nonbio degradable dyeing chemicals, can end up in wastewater. These compounds can react with conventional disinfectants, particularly chlorine, to produce a variety of disinfection byproducts that might induce allergic reactions or cancer [22]. Dye chemical structures can be altered in aquatic environments, leading to the creation of new, potentially even more dangerous chemicals. An additional environmental hazard related to dyes in surface water habitats is their high absorption of sunlight, which lowers phytoplankton's photosynthetic activity [23]. Food can be contaminated by dyes and other pollutants found in surface water. Recent research has shown that prolonged exposure to water containing dyes can seriously harm both human and animal bodies, especially the central nervous and digestive systems [24].

2.3 Rhodamine Blue dye (RhB)

Rhodamine B (RhB), a common water-soluble organic dye in the textile industry, is used in a variety of applications, including food processing, photosensitizers, water tracing, fluorescent markers for microscopic structural testing, and fabric coloring. However, because it is considered carcinogenic, its use in food processing has been prohibited for decades [41]. Additionally, because to its versatility, it is a widely used biological stain in biomedical research. However, because of industrialization and illegal release, RhB threatens human and wildlife health by contaminating fish and other food sources in water bodies that are then consumed by other species[42].Certain solvents, including butane, ethanol, and water, can be used to extract the dissolved form of RhB. It weighs 479.02 g/moll at the molecular level. The closed/no fluorescent Spiro lactam form of RhB and its open/fluorescent version coexist in balance. In an acidic environment, the "open" form is preferred, while the "closed" form stays colorless in a basic environment. At elevated temperatures, RhB fluorescence intensity diminishes [43]. RhB is made by altering xanthene molecules, which have amino and amino groups, by joining two units to create a glycoside bond [44]. Rhodamine B (RhB) dye is a synthetic dye widely used as a coloring in textiles and food products

Common name	Rhodamine B
Chemical name	[9-(2-carboxyphenyl)-6-diethylamino-3-xanthenylidene]-diethylammonium chloride
Chemical formula	$C_{28}H_{31}ClN_2O_3$
Molecular weight	479.017 g/mol
Adsorption maximum	545 nm
Class	Triphenylmethane
Appearance	Basic Violet 10; Brilliant Pink B
Molecular structure	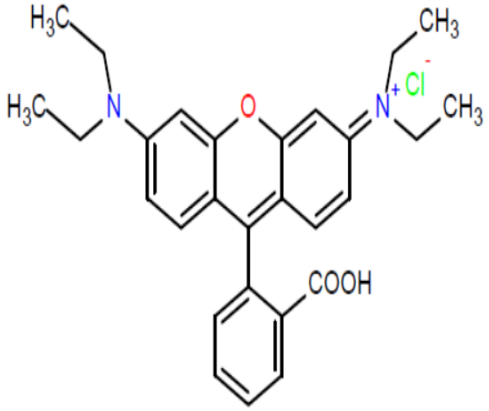

General properties of Rhodamine B [114]

2.3.1 Health and environmental effects of textile wastewater

Due to the effluents that textile factories release into water bodies, the textile industry is mostly to blame for environmental degradation worldwide. These effluents include heavy metals like copper, arsenic, plumber, cadmium, mercury, nickel, and cobalt, as well as compounds like sulfur, naphtha, vat dyes, nitrate, chromium, acetic acid, soaps, and various auxiliary chemicals that are extremely toxic and can hurt both people and animals [45]. Given their ability to transform into hazardous and cancer-causing compounds, dyes used in the textile industry present health dangers. They could have a number of harmful effects on health. Toxic substances can accumulate in the skin when the body is heated and the pores are open for absorption. The buildup of heavy metals and poisonous dyes in the body may have an impact on life and growth. Environmental dyes are absorbed chemically and biologically, prevent oxygenation, and have a tendency to trap metal ions, which accelerates micro toxicity and gene toxicity [46]. Potential pollution (toxicity or hazard

characteristics) and environmental exposure (duration and concentration) determine the dye's environmental danger. Water bodies' beauty are harmed by textile effluents. The accumulation of dyes in natural water systems reduces the amount of dissolved oxygen in the ecosystem and slows down photosynthesis by obstructing sunlight's ability to reach submerged plants and algae [47]. One type of textile effluent that has been released into the environment is RhB. It causes pain in the skin, eyes, and respiratory system and is dangerous for both humans and animals to consume. Additionally, RhB reduces light penetration, which lowers respiration and photosynthesis rates. Hazardous heavy metals are discharged into the environment during the dyes' breakdown process, when they may infiltrate the food chain and endanger people. The oxygen delivery system and the natural water bodies' self-cleaning mechanism are disrupted by the high temperature and alkaline pH of concentrated dye effluents released by textile factories following the staining process [48]. The main indicators of wastewater quality, such as suspended and dissolved particles, chemical and biological oxygen demand, and others, may be altered by dye-derived contaminants found in textile effluent. During wastewater treatment, dyes and associated compounds' durability and poor biodegradability cause numerous technological issues [25]. Modern wastewater treatment may be based on simple or hybrid physical and chemical processes like adsorption, coagulation/flocculation, chemical and electrochemical oxidation, ozonation, ion exchange, membrane process, filtration with coagulation, ozonation with coagulation and adsorption, photo catalysis, sonication, and irradiation. These days, there are two main streams of textile wastewater treatment: dyes are transferred into solid phase or sludge biomass and mineralized using methods like chemical and biological oxidation [26]. Several effective dye removal methods (such as coagulation and sorption techniques) need expensive chemicals and may produce extra hazardous waste. However, certain modern oxidation technologies (such as ozonation, Fenton's processes, electrochemical destruction, and photo catalysis) can produce nonselective hydroxyl radicals, which can be used to completely remove dye. Unfortunately, they call for somewhat intricate processes, which raises the overall cost of removing micro pollutants. Target pollutants can be fully mineralized through biodegradation, or biological decomposition processes, which is another alternate technique. Because of this technology, the overall cost of treating wastewater can be reduced. Because these techniques typically don't require harsh chemicals, they are more environmentally friendly [27].

- **Adsorption Processes**

One of the most effective and widely used purification techniques for treating wastewater is adsorption. Generally speaking, adsorption can be used in large-scale wastewater technology to eliminate colors and other organic and inorganic contaminants, including micro pollutants. Because of their great efficiency and straightforward technique, activated carbon-based compounds are the most widely utilized adsorbents. However, the limited degree of regeneration and high production cost are characteristics of these materials. Therefore, a lot of research is being done to create more effective and recyclable sorbents that could take the place of traditional active carbons [28]. Both natural and artificial ingredients, such as clay minerals, make up their composition. [29], oxides of metals [30], polymers [31], composites [32], and food waste [33]. The use of different magnetic nanomaterial's as sorbents is quite popular because of their high efficiency, which is mostly caused by their high surface-to-volume ratio, and ease of separation following the adsorption process [34].One such strategy was most recently examined by Mowed and associates[35]. The iron (II, III) oxide (Fe_3O_4)-based magnetic nanoparticles were connected with commercial polyurethane foam via isothiouronium groups. With enhanced ionic characteristics and a higher sorption affinity for ionic molecules, they created a porous sorbent. This allowed them to eliminate the liquid phase of both cationic (Brilliant Green) and anionic (Brilliant Yellow) dyes across a broad pH range of solutions. Applying an external magnetic field facilitated the quick removal of the active sorbent from the liquid phase due to the presence of magnetic particles (21.4 nm particle size) in the purification system described [35]. The experiment Wang et al. described evaluated a hybrid adsorbent [32]. They created magnetic grapheme oxide-β-cyclodextrin nanocomposites, which were effectively used to eliminate cationic dye (Malachite Green). Because of its enormous surface area and abundance of polar hydroxyl, epoxide, and carboxylic groups, grapheme oxide has been discovered to have good adsorption characteristics. Additionally, this explains why the carbon-based nanomaterial was so evenly distributed in the water. The shape and chemical structure of natural β-cyclodextrin (β-CD), another component of the hybrid sorbent described, give it a special physicochemical feature.

2.4 Biodegradation and Bio sorption Processes

An intriguing substitute for chemical technologies in wastewater dye removal is biological. They may be built on activated sludge that contains a variety of anaerobic and aerobic microorganisms, such as bacteria, fungi, and green algae. Some newer methods use more sophisticated procedures, like isolated bacterial enzymes. Currently, these technologies are being researched and used widely as effective ways to purify wastewater that contains dyes. The use of microorganism-driven purification techniques often offers a number of benefits, including low costs, minimal sludge generation, and the release of benign mineralization compounds. According to reports, dye-related contaminants can be broken down or converted by biological processes into different inorganic salts, carbon dioxide, and water. Environmentally benign biological processes can also be modified for wastewater technology procedures that adhere to stringent green chemistry guidelines [36].Both bio sorption and/or biodegradation can be used to accomplish dye bioremediation. For certain contaminants, these procedures use various removal techniques. The basis for bio sorption is the interaction between biomaterials and colorants, wherein colorants are chemically or physically affixed to the surface of biomass. A few examples of these interactions are ion exchange, chelation, surface complications, absorption, adsorption, diffusion, and precipitation. Additionally, interactions with other ligands, such as carboxylic, hydroxyl, amino, carbonyl, phosphate, and sulfonic groups that may be present on the surface of the biomaterial and dye structures are a part of dye bio sorption. Enzymes found in a variety of biomass materials made of bacteria or fungi break down pollutants during the biodegradation process. The ability of microorganisms to adapt and their activity are the two main aspects that affect how well biological dye removal works [37, 38].

Coagulation, Membrane Separation, and Oxidation Processes

It is possible to effectively purify wastewater from dyes and other contaminants using methods other than sorption or biodegradation. Specifically, methods for wastewater decolonization that were successfully studied and documented included oxidation, membrane separation, and coagulation. Polyaluminum chloride (PAC), lime, ferric or ferrous sulfate, aluminum sulfate, and other common inorganic coagulants have been proven to be efficient reagents for wastewater decolonization. However, the cost of chemicals and disposing of the sludge is the primary drawback of using these coagulants during wastewater treatment [39]. Therefore, as an alternative to inorganic coagulants, organic polyelectrolytes such as, e.g., polydiallyldimethylammonium chloride and polyamine were proposed. These compounds' technological processes are characterized by little to no extra sludge formation. The overall cost of the decolonization procedures may be considerably reduced because it has been shown that the total volume of these reagents can be substantially lower than that of inorganic coagulants. Nearly all dye pollutants have demonstrated minimal sensitivity to polyelectrolytes' pH range of 3 to 10. For a consistent removal rate, coagulation utilizing inorganic coagulants necessitates limited and stable pH settings (pH = 5 for PAC, for example). By using inexpensive carboxylate surfactants in conjunction with ionic flocculation, process costs can be further decreased. They are easily obtained by using sodium hydroxide to saponify vegetable and/or animal fats [40].

➢ Adsorbent materials

❖ Adsorption by carbon-based material

Many adsorbents have been utilized recently to remove various dyes, including RhB dye. Activated carbon stood out among those adsorbents for a number of reasons. Its increased adsorption ability in wastewater treatment with organic dye molecules is due to its high surface area, porosity, and chemical characteristics [61]. Fruit peels, sugar, beans, and zeolites are the main sources of carbon adsorbents [62]. The fact that carbon exists in a variety of forms is due to its distinct electronic structure, which permits the creation of stable chemical bonds in a range of configurations. The capacity to generate single, double, or triple bonds, as well as to catenae (bind with one another) to form cyclic or acyclic chains, straight or branching chains, and bonds with other on-metallic elements, are what make carbon special [115].

❖ **Adsorption by noble material**

Gold, rhodium, palladium, platinum, and other noble metals are resistant to heat and chemicals. They are employed in the manufacturing of automobile exhaust gas converters because of their special qualities [113]. Metals with a negative redox potential can lower the positive redox potential of noble metals. It is possible to extract noble metals from solutions using the cementation method. Through cementation with iron powder, gold thiocyanate complexes were extracted from a thiocyanate solution [114]. The precipitation of ammonium hexachloroplatinate can be used to extract platinum [115]. Platinum has been extracted from a chloride solution using a similar precipitation technique [116]. The positive redox potential of noble metals can be diminished by metals with a negative redox potential. Using iron powder for cementation, gold thiocyanate complexes were extracted from a thiocyanate solution [117]. Organic acids like oxalic acid and zinc can both degrade gold. In addition to precipitation, precious metals can be separated using solvent extraction. In hydrochloric acid solutions (0.59M), gold(III) ions were separated from platinum(IV), palladium(II), rhodium(III), and iridium(III) using Cyanic 272 (bis(2,4,4-trimethylpentyl)phosphine acid) [118].In a concentrated 6M hydrochloric acid solution, palladium (II) ions were isolated from platinum (II), rhodium (III), and iridium (III) using LIX63 (5,8-diethyl-7-hydroxydodecane-6-oxime) [119].

❖ **Adsorption based on metal oxide**

Metal oxides are the most generally utilized surfaces for removing pollutants because they are inexpensive, easily produced, and have superior mechanical qualities and resilience to thermal degradation when compared to biological surfaces [119].One of the most well-known oxides is aluminum oxide (Al2O3), an amphoteric oxide also referred to as alumina that is present in a variety of crystalline formations such as "α-Al2O3, γ-Al2O3, θ-Al2O3, η-Al2O3," etc., each with unique physical and chemical characteristics and uses [120]. Aluminum oxide is an effective adsorbent due to its numerous hydroxide groups, ease of usage, chemical stability, and non-toxicity. Aluminum oxide has been used as an adsorption material since 1923 to eliminate pigments, medicines, heavy metals, and dissolved organic [121].

❖ Adsorption based on transition metal

The transition metals exhibit magnetic characteristics and the unique ability to generate colorful compounds. There are numerous industrial uses for metals derived from the D-block. They function as phosphors, ceramics, sensors, super conducting materials, catalysts, and crystalline lasers etc. In the battery and chemical industries, transition metals and their compounds are employed as catalysts. In addition, these compounds are good photoactive materials that operate as photosensitizers and can be employed to build interstitial compounds and alloys. Devices having beneficial qualities for chemical electrolysis are mixed metal oxide (MMO) electrodes. The name describes electrodes that have two different types of metal oxides on their surface. One type is often RuO2 and IrO2, which can react to produce chlorine gas. Titanium dioxide, the other metal oxide, is usually less expensive and stops internal corrosion, but it neither conducts nor catalyzes the reaction. Titanium is usually used to make the electrodes inside. Approximately 10 to 12 grams of precious metal (apart from titanium) can be found per square meter. FeO (wastage), Fe3O4 (magnetite), Fe2O3 (hematite), and Fe2O3 (magnetite) are among the phases that are formed by Fe and O. While the remaining oxides are found in nature, the final phase is synthetic. The Fe-O phase diagram indicates that, in the majority of temperature and pressure preparation circumstances, the Fe2O3 stoichiometry predominates [1]. Numerous studies have been conducted on the magnetic characteristics of iron oxides, specifically on the enhancement of magnetic recording properties for nanostructure materials or the application of magnetite in Fe2O3-SiO2 composite materials with magneto-optical properties. The majority of physio-chemical investigations focus on the gamma (cubic inverse spinel) and alpha (corundum structure with a deformed hexagonal anion closed-packed). © 2017 JETIR April 2017, Issue 4, Volume 4, www.jetir.org (ISSN-2349-5162) Journal of Emerging Technologies and Innovative Research (JETIR) 1704088 www.jetir.org 398 distinct stages. Although the size stability of the polymorphs has been investigated, there is still disagreement on a broad range of topics, especially those pertaining to the presence of nanoparticles with alpha structures. Adsorbents: Arias et al [2].

2.5 Polyaniline-based nanocomposites for water and wastewater treatment

A class of novel materials for adsorption, polymers have high surface areas, variable surface chemistry, superior mechanical stiffness, a desired distribution of pore sizes, and cost-effective regeneration in mild environments [49]. PANI is a conducting polymer that has been thoroughly investigated as a potential adsorbent for the removal of aqueous pollutants because of its distinct electrical properties, ease of synthesis, inexpensive monomer costs, outstanding environmental stability, easily controlled reversible properties (e.g. by charge exchange doping and protonation), distinct functional groups (e.g. NH–), and adjustable properties [50]. Furthermore, PANI-based nanocomposites have been extensively researched for the adsorption of pollutants because of their high surface areas, superior dispensability, and the synergistic qualities of the filler and polymer [51]. PANI-based nanocomposites also have the advantage of having a variety of morphological morphologies that may be altered by varying synthesis parameters like temperature, reaction time, and dopant type. Thus, to remove aqueous contaminants (such as heavy metals and dyes), PANI-based nanocomposites with different nanostructures have been created [52].

2.6 Synthesis and characterization of PANI-based adsorbents

PANI can be produced through chemical oxidation [53] or electrochemical oxidation [54] polymerization of aniline more frequently, PANI is created by chemically oxidative polymerizing aniline using free radical initiators like ferric chloride, potassium dichromate, ammonium peroxydisulfate, potassium per sulfate, and chloroaurate as oxidants [55]. The three primary processes of chemical polymerization of aniline by oxidation are initiation, chain propagation, and termination using a radical dominating mechanism. The aqueous solution of aniline can be electrochemically polymerized by (1) applying a constant current (galvanostatic), (2) applying a constant potential (potentiostatic), or (3) applying a potential scanning/cycling [51]. In a strongly acidic aqueous electrolyte, electrochemical polymerization is usually carried out via a radical polymerization process, which forms anilinium radical actions by aniline oxidation on the electrode [56]. The primary method for creating PANI-based adsorbents is in-situ polymerization with organic or inorganic fillers, which results in better filler dispersion and less PANI molecule aggregation [57 To improve adsorption performance, PANI has been modified to accommodate a range of adsorbents with distinct properties. Chemical oxidation can be used to create PANI and PANI-based adsorbents. To improve adsorption performance, PANI has been modified to

accommodate a range of adsorbents with distinct properties. Chemical oxidation can be used to create PANI and PANI-based adsorbents [53]. Or electrochemical oxidation [54]. Aniline polymerization. These adsorbents are frequently created by producing PANI hollow microspheres using the in-situ chemical oxidative polymerization of aniline by free radical initiators spheres in solvents. Emulsion polymerization was used by Liu et al. to create mono dispersed poly (styrene-methyl methacrylate-acrylic acid) microspheres, then in-situ polymerization was used to coat PANI onto the microspheres [58]. Both surface areas and adsorption capacities of the PANI-coated microspheres rose from 22.8 to 41.7 m2/g and 140 to 155 mg/g, respectively. Research interest in magnetic nanoparticles for wastewater color removal is developing. The magnetic core of magnetic mesoporous nanocomposites, in particular, has strong magnetic interactions, but the polymeric shell contains functional groups that preserve the adsorbent pore size distribution and stop magnetic metal compounds from clumping together [59].After creating chitosan-functionalized magnetic microspheres (Fe3O4@CHI) using a co-precipitation technique, Jiang et al. created Fe3O4@CHI@PANI microspheres with core–shell structures (core diameter 20–30 nm) and uniform sizes at ~100 nm by polymerizing aniline on the magnetic core's surface. [60]. Low-cost bio adsorbents like chitosan are also frequently included into the traditional in-situ chemical oxidative polymerization synthesis process [61] .and agriculture wastes [62] .Into PANI to offer a large number of functional groups and adsorption-friendly surface regions. Using a modified in-situ oxidative polymerization technique, Alshammari et al. created chitosan-graft-substituted PANI with the use of ultra-sonication [63].

2.7 Magnetite (Fe_3O_4) nanoparticles

These days, nanosized magnetic magnetite (Fe3O4) particles are investigated extensively in a wide range of scientific fields, both fundamentally and practically, primarily due to their special and adjustable magnetic characteristics that can meet the requirements for a variety of applications [64]. Among the readily accessible and cheaply produced naturally occurring iron oxides is magnetite. The chemical formula of FeO.Fe2O3 indicates that Fe3O4 nanoparticles generally have ferromagnetic characteristics in bulk, with a high Curie temperature (Tc) of 577°C and a high magnetization saturation (MS) of 92 emu/g at ambient temperature. However, the size of the Fe3O4 nanoparticles controls their magnetic characteristics. When ferromagnetic Fe3O4 nanoparticles are tiny enough, they exhibit superparamagnetic characteristics and react strongly to applied magnetic fields[65].The majority of iron oxides,

including goethite, hematite, lepidocrocite, and magnetite, are semiconductors, although magnetite has characteristics more like to those of a metal. Several pollutants, including carbon tetrachloride (CCl4), hexavalent uranium (U6+), and chromium Cr6+, have also been demonstrated in lab experiments to be reduced by magnetite. The magnetic property and color of magnetite are due to its inverse spinel crystal structure, which has a unit cell of 32 oxygen atoms in a face-centered cubic structure with a unit cell edge length of 0.839nm.Its crystal structure's intervalence charge transfer between Fe2+ and Fe3+ is what causes the black cooler. The tetra and octahedral locations of the Fe2+ and Fe3+ atoms, as previously mentioned, are another source of magnetite's magnetic properties. The tetrahedral and octahedral sites have antiparallel spins, with differing magnitudes for each type of spin. Magnetite is converted to maghemite or hematite in an oxidizing environment [66].

2.7.1 Synthesis of magnetite (Fe_3O_4) nanoparticles

To properly manage the particle's size, shape, crystallinity, and magnetic characteristics, a substantial amount of research has been conducted in the past 20 years to create magnetic Fe3O4 nanoparticles [64].Physical, chemical, and biological approaches are the three most significant documented pathways for the creation of Fe3O4 nanoparticles to date. Because it is simpler, more efficient, biocompatible, nontoxic, and reproducible than other synthetic approaches, a biological green synthesis method is recommended [64]. In addition, because the green synthesis method doesn't require pricey tools or chemicals, it's a quicker and more economical way to create nanoparticles. An understanding of the mechanism, process, and influencing aspects of the procedures used to synthesize nanoparticles is crucial for controlling and optimizing their attributes, including size distribution, crystal structure, magnetic properties, and particle size

2.6.2 Green synthesis of magnetite nanoparticles

In general, "green synthesis" refers to the production of Fe3O4 nanoparticles or nanomaterial’s without the use of dangerous chemicals that result in toxic byproducts. To put it another way, the green method is an environmentally benign way to create nanoparticles that doesn't endanger human health or the environment. The biological substances found in green materials have the potential to stabilize the nanoparticles during the manufacturing process by acting as capping and reducing agents. This allows the nanoparticles' size and form to be controlled for a variety of uses

[67].Although there are numerous successful studies that demonstrate the synthesis of Fe3O4 NPs via various biological pathways, plant extract is most frequently utilized in green synthesis due to its ease of acquisition, large-scale production, affordability, and environmental friendliness. Moreover, plant extracts may function as stabilizing and reducing agents during the creation of nanoparticles, possibly as a result of phytochemicals. Phytochemicals are substances that the body produces on its own [68].

2.8 Photochemistry of *Croton macrostachyus* (Bisana) plant

The *macrostachyus Croton* Hoechst. Ex Delile belongs to the Euphorbiaceous family, also referred to as the spurge family, and is a species of the genus Croton L. A medium-sized, drought-deciduous pioneer tree, *Croton macrostachyus* grows naturally in less productive locations such as waste grounds, mountain slopes, and forest borders under a variety of ecological circumstances [69].Since *Croton macrostachyus* is frequently cultivated and maintained in home gardens to provide a variety of ecosystem goods and services, subsistence farmers in Ethiopia, Kenya, and Tanzania view it as a multipurpose tree. For instance, in mid-altitude and semi-arid regions of Ethiopia, *C. macrostachyus* is a significant tree intercropped in agro-ecosystems to boost soil production [70].The pharmacological characteristics and therapeutic applications of C. macrostachyus are also of great interest across its tropical African distributional region. According to the research conducted by these authors, C. macrostachyus is a significant medicinal plant in tropical Africa that has the potential to produce significant pharmaceutical products for use by both urban and rural groups that depend on herbal drugs for basic healthcare. The World Health Organization (WHO) has advised combining traditional and contemporary medicine, mostly because both impoverished rural and urban groups as well as those residing in disadvantaged areas believe that traditional remedies are more accessible, economical, and acceptable [71]. Given the ethno medical applications of *C. macrostachyus* that have been described in tropical Africa, there is no doubt that the species has the potential to play a significant role in the primary healthcare of communities across its region of distribution. Several classes of phytochemicals have been identified from the fruits, leaves, stem bark, and twigs *of C. macrostachyus*, including alkaloids, amino acids, anthraquinones, carbohydrates, cardiac glycosides, coumarins, essential oil, fatty acids, flavonoids, phenolic compounds, phlobatannins, polyphenols, phytosteroides, saponins, sterols, tannins, terpenoids, unsaturated sterol, vitamin C, and

withanoides [72, 73].When creating nanoparticles, this primary and secondary metabolite is employed as a capping and reducing agent. *Croton macrostachyus* plant leaf extract was chosen for our thesis PANI/Fe3O4 adsorbent green synthesis since no other researcher had previously used this plan leaf for these composite synthesis.

2.9 Removal Methods by using Magnetite from Wastewater

In order to create nanoadsorbents or materials with the appropriate quality and properties to remove these harmful contaminants from wastewater, nanotechnology is currently thought to be comparatively better and superior. They have large surface area, porosity, adjustable reactivity, and suitable dispensability due to their small size. They can be distributed properly. Nanoparticles may move through soil like water when properly prepared and stabilized, and they can rapidly examine enormous amounts when in the liquid phase. It's likely possible to adjust their reactivity so that it attacks both organic and inorganic molecules, but not biological forms [74].Iron, nickel, cobalt, and other magnetic elements, as well as their oxides, such as magnetite (Fe2O3), magnetite (Fe3O4), cobalt ferrite (CoFe2O4), nickel ferrite (NiFe2O4), etc., are typically the components of metallic nanoparticles. The inorganic components (gold, platinum, cobalt oxide, aluminum oxide, silica, and activated carbon) or organic layers (polymers or surfactants, including polyethylene glycol and dextran) are typically used to cap metallic nanoparticles (NPs) to render them stable against oxidation, corrosion, and aggregation. For this reason, nanotechnology is currently regarded as a cutting-edge concept with potential applications in biomedicine and the environment [75].

2.9.1 **Adsorption**

The surface phenomena of adsorption has a common mechanism for the removal of both organic and inorganic contaminants. Some solute molecules from the solution are concentrated or deposited at the solid surface when a solution containing absorbable solute comes into contact with a solid having a highly porous surface structure due to liquid-liquid intermolecular forces of attraction. Adsorbent is the surface on which accumulation takes place, while adsorb ate is the substance that builds up on the surface .It falls into two categories: chemical and physical adsorption. Adsorbent and adsorb ate interact chemically or biochemically during chemical adsorption, also known as chemisorption. Chemical adsorption is typically an irreversible process and is found to be highly efficient. In physical adsorption, the accumulation of mass because of weak attractive Vander Waals forces, hydrogen bonding,

polar-polar interaction, etc., and the process is reversible in most cases. Apart from the removal of dyes adsorption, using the chemical adsorption approach is widely used for removing heavy, toxic, or preciousmetals, anionic groups, toxic organic compounds, and pollutants. Other techniques are usually not attractive due to their high operation costs and the time consuming processes involved [76].

2.8.1 PANI -based adsorbent for dye removal

PANI, a highly naturally conductive polymer, has drawn more attention in the dye removal field because of its low cost, high surface area, ease of use, environmental and thermal stability, and—above all—its unique electro activity, which offers remarkable desorption efficiency. In a number of aspects, the nanocrystal line structure of PANI—which includes nanofibers, Nano rods, nanowires, and nanotubes—has sparked attention and improved performance. This is why PANI and several transition-metal oxide polymeric nanocomposites, including PANI/ZnO, PANI/SnO2, PANI/ZrO2, PANI/CeO2, PANI/TiO2, PANI/rGO, PANI/SiO2, and PANI/Fe3O4, [78, 79] used as organic dye adsorbents until recently .The adsorption-based process is thought to be a better method in terms of cost, adaptability, ease of design and operation, and insensitivity to toxic contaminants. It produces a high-quality effluent without causing any additional hazardous material development. The development of inexpensive, eco-friendly, and generable adsorbent nanoparticles is the primary goal of adsorption-based nanotechnology, which aims to remove pollutants from wastewater efficiently [80].

2.9 Factor affecting adsorption

2.9.1 Effects of solution pH

The dye solution's pH has a significant impact on both the adsorption capacity and the entire adsorption process. As the pH of the solution rises, removal efficiency increases until equilibrium is achieved. A charge is frequently formed on the adsorbent surface ahead of the deprotonating reaction due to the very fact that rising pH causes this. High removal efficiency is made possible by this charge because of the electrostatic interaction between the charged adsorb ate and the adsorbent; at lower pH, however, the reactive atom and different functional groups of when the adsorbent protonated, both became charged. The electrostatic repulsion and growing competitive

effect of OH-ions for the sorbent's active sites may have an impact on RHB adsorption at higher pH. Because of its positive charge, the sorbent surface promotes the anions' adsorption [81]. Thus, the adsorption of RhB with an initial dye concentration of 10 _mol/L was studied by adjusting thesolution pH from 2 to 10, and the results are presented in Figure

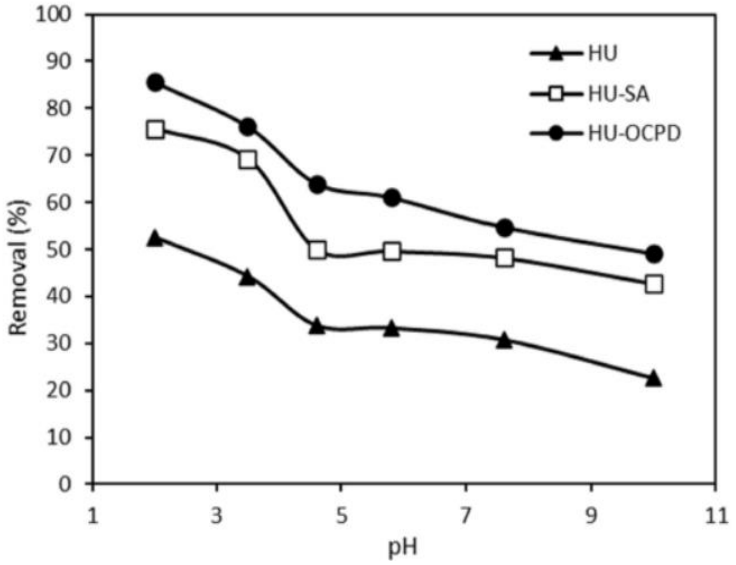

Effect of solution pH on the adsorptive removal of RhB dye[124]

2.9.2 Effect of adsorbent dosage

One important factor that influences the quantity of adsorbed adsorb ate is the ideal adsorbent dose. As the dosage of the adsorbent is increased, the surface area increases. Determining the ideal dosage is essential to prevent ingesting too much adsorbent. By changing the adsorbent dosage concentration, a number of study teams have examined the impact of adsorbent dosage. Because there are more accessible active sites in the adsorbent, removal efficiency typically increases as adsorbent dosage increases. However, the adsorption capacity stays constant after a specific dosage of the adsorbent. This constant is typically caused by the abundance of accessible surface-active groups relative to the amount of adsorb ate [82].

2.9.3 Effect of contact time

Contact time has a big impact on the adsorption process. Both the process's economic efficiency and the adsorption kinetics can be impacted by contact time. Thus, another performance controlling factor in the adsorption process is contact time. According to earlier research, adsorption typically happens in three stages: quick adsorption at first, followed by slow adsorption,

and equilibrium state adsorption, which is reached and stays constant. Rapid adsorb ate molecule attachment to the surface adsorbent via surface mass transfer may be the cause of the first step's high adsorption capacity. The delayed second step is most likely connected to the first phase's occupation of the external sites that were available. In the third stage, the available adsorption sites finally become few, resulting in the equilibrium state. The delayed second step is most likely connected to the first phase's occupation of the external sites that were available. In the third stage, the available adsorption sites finally become few, resulting in the equilibrium state [82].

2.9.4 Effect of initial concentration

The pollutant removal effectiveness of an adsorbent that depends on the combination of pollutant concentration and accessible binding sites on the adsorbent surface can be changed by the initial concentration of dyes in the solution. The necessary driving force to suppress the mass transfer resistance of the pollutant between the liquid polluted water phase and the solid adsorbent can be found in the initial concentration of the pollutant [81].

2.9.5Adsorption isotherm study

Adsorption isotherms provide a detailed insight of the nature of the interaction between the adsorbent and the adsorbate. Isotherms aid in providing data regarding the best way to use adsorbents. Isotherm curves are very important since it offers details on the interaction processes and maximum adsorption capacity of a specific adsorbent, which is useful for adsorption purposes [83].

2.9.6 Langmuir isotherm model

The fundamental premise is that certain homogenous locations inside the adsorbent are where the sorption occurs [83]. The Langmuir isotherm is given by the following equation: 1

$$\frac{C_e}{q_e} = \frac{1}{bqm} + \frac{C_e}{q_m} \ldots\ldots\ldots\ldots\ldots\ldots\ldots\ldots\ldots\ldots\ldots\ldots\ldots\ldots\ldots\ldots\ldots\ldots\ldots\ldots\ldots\ldots\ldots\ldots\ldots\ldots\ldots\ldots\ldots\ldots\ldots (Eq1)$$

Where b is a constant (L mmol-1) for the Langmuir isotherm, Ce is the solute's equilibrium concentration (moll L-1), qe is the quantity of solute adsorbed per unit weight of adsorbent (mmol g-1 of adsorb ate), and qm is the adsorption capacity (moll g-1), also known as the monolayer capacity.

For the Langmuir isotherm, the isotherm curves were plotted Ce/qe against Ce. [83].

2.9.7 Freundlich isotherm model

Assuming a heterogeneous surface with an uneven distribution of heat of adsorption throughout the surface, the Freundlich isotherm is obtained. The Freundlich isotherm model's mathematical expression is:

$$= logK_f + \frac{\log Ce}{n} \ldots\ldots\ldots\ldots\ldots\ldots\ldots\ldots\ldots\ldots\ldots\ldots\ldots\ldots\ldots\ldots\ldots\ldots\ldots\ldots\ldots\ldots\ldots\ldots\ldots\ldots\ldots (Eq2)$$

Where Kf and n are empirical constants, Ce is the solute concentration (mmol L-1), and qe is the quantity of solute (log) _adsorbed per unit weight of adsorbent (mmol g-1 of adsorb ate). The Freundlich isotherm model's isotherm curves are displayed as log qe vs log Ce graph [83].

2.9.8 Adsorption kinetics study

The experimental data has been analyzed using various kinetic models in order to identify the rate-limiting stage during the adsorption process. These models include pseudo-second-order and first-order models.

2.9.9 Pseudo-First order model

The link between the rate at the occupied sorption sites of the adsorbents and the number of vacant sites is explained by the pseudo-first-order (PSO) kinetic model. It has the following definition based on Lagergren's equation [84]:

$$lan(q_e - q_t) = lnq_e - k_1 * t \ldots\ldots\ldots\ldots\ldots\ldots\ldots\ldots\ldots\ldots\ldots\ldots\ldots\ldots\ldots\ldots\ldots\ldots\ldots\ldots\ldots\ldots\ldots\ldots.. (Eq3)$$

2.10 Pseudo-second order modeling

The pseudo-second-order model visualizes chemisorption as the rate-controlling step and is based on the solid phase's adsorption capacity. The following equation represents the pseudo-second-order kinetic in linear form:

$$\frac{1}{q_t} = \frac{1}{K_2 q_e^2} + \frac{1}{q_e\, t} \ldots\ldots\ldots\ldots\ldots\ldots\ldots\ldots\ldots\ldots\ldots\ldots\ldots\ldots\ldots\ldots\ldots\ldots\ldots\ldots\ldots\ldots\ldots\ldots\ldots\ldots. (Eq4)$$

Where qe (mg/g) is the amount adsorbed at equilibrium time; qt (mg/g) is the amount adsorbed at a time, t (min); K2 is the pseudo-second-order rate constant. The kinetic rate constant, k, and qe for each model can be calculated by plotting graph log t/qt versus t for pseudo-second-order models [84].

CHAPTER THREE
3 Material and Methods

3.1 Materials and Equipment's

An analytical balance, mortar and pestle, 250-ml plastic bottles, magnetic stirrer, sieves (200-250mm size), pH meter, 50-250ml-size beaker, measuring cylinder, conical flask, digital oven, stir bar, UV-DRS (UV-Vis NIR CLB, Model V-770), ATR-FTIR (Perkin Elmer spectrum 65 model FTIR), P-XRD (XRD-7000, SHIMADZU Corporation, Japan), crucible, volumetric flasks (50-250 ml), test tubes, gloves, and what man filter paper, among other important tools and apparatus used in this thesis.

The majority of the chemicals used in this thesis project were laboratory-grade analytical chemicals that were acquired from several chemical suppliers. The following substances were employed in this thesis study: ethanol (CH3CH2OH), sodium hydroxide (NaOH), aniline, ammonium per sulfate, distilled water, tap water, iron (III) chloride hex hydrate (FeCl3.6H2O), and iron (II) chloride tetra hydrate (FeCl2.4H2O)(H2O).

3.2 Chemicals and reagents

3.3 Experimental site

In order to construct a composite adsorbent sample, green plants (*Croton macrostachyus*) were collected from multiple locations in Wolkite City, Ethiopia. The PANI/magnetite adsorbent was synthesized and all batch adsorption studies were carried out at the Department of Chemistry Laboratories at Wolkite University.

3.4 Experimental Design and Procedures

3.4.1 Collection of *Croton macrostachyus* Plant Leaf

The leaf litter of *Croton macrostachyus*, also referred to as Bisana locally, was gathered from the Wolkite town in Ethiopia's Gurage zone for this study. The collected leaves were rinsed with distilled water after being properly cleansed with tap water multiple times to get rid of any pollutants. Following cleaning, the leaves were allowed to air dry in a shaded area away from direct sunshine, preventing heat or moisture-induced deterioration for around 15 days. After drying, an electrical grinder was used to grind the leaves into a fine powder. After processing, this

powder was kept in storage to be used as a reducing agent in the environmentally friendly synthesis of nanoparticles in the extraction and synthesis processes that followed.

3.4.2 Preparation of Leaf Extract in *Croton macrostachyus* plants

Freshly harvested leaves were obtained from Wolkite town for this section of the investigation. The leaves were completely washed with distilled water to guarantee they were pure and devoid of any impurities or dirt. Following their cleaning, the leaves were left to air dry at room temperature. The leaves were dried and then powdered into a fine powder so that the active ingredients could be extracted more easily .After that, 200 mL of distilled water was combined with 5.0 g of powdered *Croton macrostachyus* leaves, and the mixture was brought to a boil at 50°C for an hour. The phytochemicals, which serve as reducing agents in the creation of nanoparticles, must be extracted from the leaves using this heating method. The liquid was brought to a boil and then allowed to cool to room temperature. The extract was filtered twice through what man filter paper to get rid of any remaining plant matter or trash. To maintain its active qualities until it was required for the nanoparticle manufacturing procedure, the filtered extract was thereafter kept in a refrigerator at 4°C. Later on, this extract would be used as the stabilizing and reducing agent for the environmentally friendly synthesis of the PANI/FeO_4 adsorbent.

3.4.3 Synthesis of polyaniline nanoparticles

An extensively utilized process for creating conducting polymers, oxidative polymerization, was employed to create polyaniline (PANI). The procedure started by dissolving 15 mL of aniline monomer in 335 mL of 1.5 M hydrochloric acid (HCl) to create the monomer solution. The aniline must be protonated in an acidic solution in order for polymerization to take place and the monomer to be in the proper ionic form. A further 335 milliliters of 1.5 M HCl were used to dissolve 25 grams of ammonium per sulfate (APS) powder in order to create an initiator solution. Ammonium per sulfate is a potent oxidizing agent that creates the ideal oxidative environment for the polymerization of aniline monomer into polyaniline. After that, the aniline monomer solution and the APS initiator solution were mixed together in a glass reactor and allowed to sit at room temperature for eight hours. Stirring the fluid facilitates the polymerization reaction and guarantees that the reactants are distributed uniformly. Maintaining a homogenous reaction mixture during the polymerization process required careful management of the solutions' flow rate since irregular

mixing could result in the creation of non-uniform polymer chains. Over the course of the process, the solution's color progressively shifted from pale yellow to a greenish-black hue. Given that the typical greenish-black hue is indicative of the emeraldine base form of polyaniline, a common and stable oxidation state of the polymer, this color shift is an obvious sign that PANI nanoparticles have successfully formed. Maintaining a homogenous reaction mixture during the polymerization process required careful management of the solutions' flow rate since irregular mixing could result in the creation of non-uniform polymer chains. Over the course of the process, the solution's color progressively shifted from pale yellow to a greenish-black hue. Given that the typical greenish-black hue is indicative of the emeraldine base form of polyaniline, a common and stable oxidation state of the polymer, this color shift is an obvious sign that PANI nanoparticles have successfully formed [85]. The mechanism of polymerization of aniline by ammonium persulfate ware.

Propagation of Chain

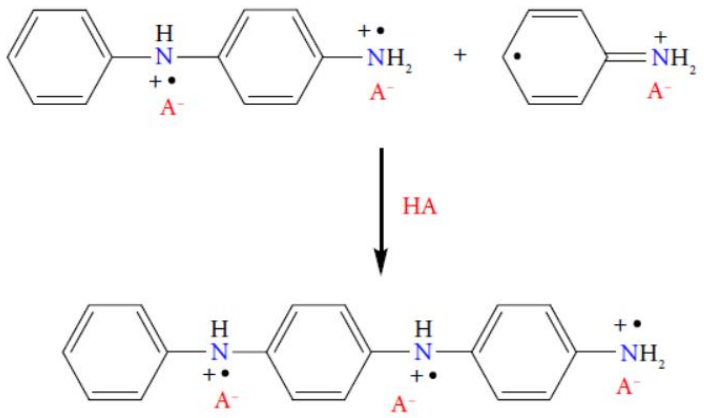

Reduction of Propagation of Chain

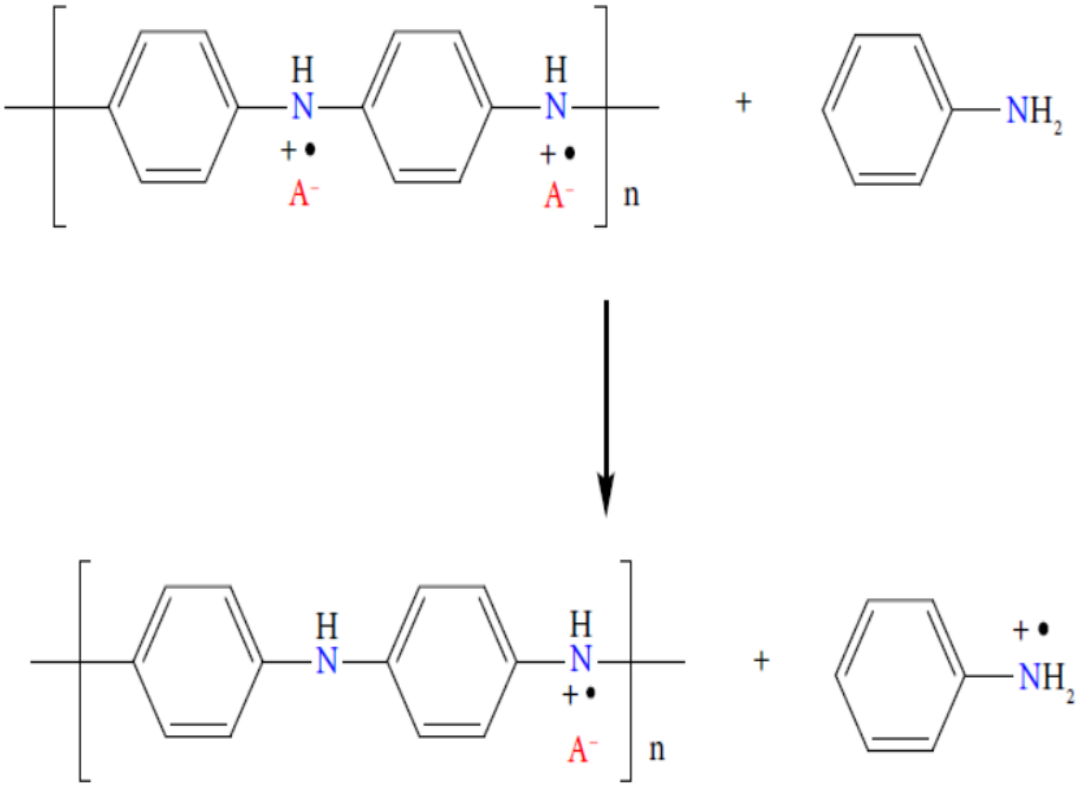

Chemical (oxidative) polymerization of aniline [113].

3.4.1 Synthesis of magnetite NPs Using *Croton macrostachyus* Leaf Extract

The co-precipitation method, a straightforward and efficient way to create magnetic nanoparticles, was used to create magnetite (FeO_4) nanoparticles. 2.65 g of ferrous chloride tetra hydrate ($FeCl_2•4H_2O$) and 5.3 g of ferric chloride hex hydrate ($FeCl_3•6H_2O$) were first dissolved in 500 mL of distilled water to start the manufacturing process. To guarantee that the salts were completely dissolved, this solution was then heated to 80°C on a hot plate while being gently stirred by a magnetic stirrer. As is common for a mixture of ferrous and ferric ions in solution, the resultant solution was light orange in color.100 mL of the *Croton macrostachyus* leaf extract was added to the mixture after the salts had completely dissolved. Rich in flavonoids and polyphenols, the leaf extract performed two roles during the synthesis process: it acted as a stabilizing or capping agent to avoid the agglomeration of the resultant nanoparticles and as a reducing agent to promote the reduction of iron ions. Continued stirring after the leaf extract was added resulted in a

discernible change in the solution's hue. The mixture's light orange tint changed to a brownish-black hue after roughly five minutes, signifying the development of magnetite iron oxide nanoparticles. After that, 20 milliliters of 1 M sodium hydroxide (NaOH) was added to the mixture in order to raise the pH and cause magnetite (FeO_4) nanoparticles to precipitate. The solution became more basic as a result of the NaOH, and black magnetite precipitates formed. To guarantee that all of the iron oxide precipitated, the mixture was agitated for five more minutes. At this point, the development of the black precipitates showed that the magnetite nanoparticle production was successful. After removing the solution from the hot plate, the precipitate was given time to settle. Centrifugation was used to remove excess reagents and any unreacted material from the precipitate in order to separate the magnetite nanoparticles. To make sure the nanoparticles were pure, this washing process was carried out five times. Following washing, the precipitate was meticulously dried for eight hours at 80°C in a hot air oven to eliminate any last traces of moisture and further solidify the nanoparticles. To keep the dried magnetite nanoparticles safe from moisture and contamination, they were kept in a hermetically sealed jar. These magnetic magnetite nanoparticles were then prepared for characterization and further application in the creation of nanocomposites, including the hybrid PANI/FeO_4. For the production of magnetite nanoparticles with potential uses in drug delivery, wastewater treatment, and catalysis, the co-precipitation method in conjunction with the green synthesis approach employing *Croton macrostachyus* leaf extract offers a sustainable, economical, and ecologically friendly method [86].

3.4.4 Synthesis of PANI/Fe_3O_4 adsorbent

In order to produce adsorbent material with improved qualities, different weight percentages of FeO_4 nanoparticles were added to polyaniline (PANI) during the sol-gel production of PANI/FeO_4 adsorbent. To create the basic monomer solution for polymerization, 10 mL of 1.5 M hydrochloric acid (HCl) and 5 mL of aniline monomer were mixed to create an acidic solution. Ethylene glycol, which served as a solvent and stabilizer, was then added to the mixture in an amount of 60 milliliters. Ethylene glycol facilitates improved homogeneity by spreading the nanoparticles inside the matrix. After that, different amounts of the previously manufactured FeO_4 nanoparticles—between 5% and 20 percent by weight—were added to the mixture. This range enables the examination of the impact of varying FeO_4 concentrations on the final nanocomposite characteristics. To make sure the iron oxide nanoparticles were evenly distributed throughout the ethylene glycol solution and formed a sol, the mixture was magnetically agitated for 30 minutes at

50°C.Ten milliliters of an aqueous ammonium peroxydisulfate (APS) solution were added to the sol to start the polymerization of aniline. In order to convert the aniline monomer into polyaniline, APS acted as an oxidizing agent. For five hours, magnetic stirring was applied to the resultant reaction mixture at temperatures between 80 and 90°C. This stage encouraged aniline's oxidative polymerization, which caused the sol to progressively change into a gel. For the polymerization rate to be regulated, well-structured PANI to develop, and the FeO_4 nanoparticles to successfully integrate into the polymer matrix, the reaction temperature is essential. The gel was given a 24-hour aging period following polymerization in order to solidify and achieve its ideal structure. After that, the aged gel was cautiously put on glass substrates so that it could be examined further. To describe the morphology, chemical structure, and crystallinity of the PANI/FeO_4 nanocomposites, these examinations may employ methods like X-ray diffraction (XRD), Fourier transform infrared (FTIR) spectroscopy, and others. The sol-gel process provides a practical way to create adsorbent with evenly distributed nanoparticles that may be customized for a range of uses, such as environmental remediation, sensors, and catalysis. By altering the proportion of FeO_4 nanoparticles by weight, the study probably investigated how adding magnetic nanoparticles impacted the PANI matrix's mechanical strength, electrical conductivity, and adsorption capacity, making it a very adaptable composite for a variety of technological uses [85, 86].

3.5 Phytochemicals tests of *Croton macrostachyus* leaf extract

Croton macrostachyus leaf extracts were tested for flavonoids, tannins, coumarins, saponosid, glycosides, anthocyanin, terpenoids, and phenols. Aqueous solution of the material was prepared using the procedure described in [87],

3.5.1 Test of coumarins (Alkaline reagent test)

In a test tube, two milliliters of NaOH and two milliliters of the *Croton macrostachyus* extract solution were mixed together. The appearance of blue or greenish-yellow fluorescence indicated a positive outcome for coumarins [87].

3.5.2 Test of Tannins

Drops of diluted ferric chloride solution (0.1%) were added after 2 mL of *Croton macrostachyus* extract solution was added to 2 mL of water. Positive signs include a green to blue-green hue (catechuic tannins) or a blue-black coloration (garlic tannins) [88].

3.5.3 **Test for Glycosides**

One milliliter of distilled water was also combined with an aqueous NaOH solution, which was then added to a little quantity of extract that had been dissolved in the latter. The presence of glycosides is indicated by the reddish-brown hue [87].

3.5.4 **Test for flavonoids**

Additionally, a small amount of extract was diluted in one milliliter of distilled water, and an aqueous NaOH solution was added. A reddish-brown hue that indicates the presence of glycosides [87].

3.5.5 Test of phenols

When 1 mL of *Croton macrostachyus* extract solution was treated with drops of ferric chloride (5%) and watched for the development of deep blue or black hues, a positive test for the phenol group was obtained [88].

3.5.6 **Test for saponins**

0.2 mL extract were mixed with 2.0 mL distilled water, shaken for 20 min and the persistence of foams indicated the presence of saponins [88].

3.5.7 **Test for steroids**

Along the test tube walls, two milliliters of extract, one milliliter of chloroform, and one milliliter of pure H2SO4 acid were carefully added. When the combination was inspected, the chloroform layer showed a red hue, indicating the presence of steroids [88].

3.5.8 Test of terpenoids (Chloroform test)

Two milliliters of chloroform and two milliliters of plant extract solutions are combined to perform the terpenoids test. Then, using 2 mL of concentrated H2SO4, this mixture was heated for 120 seconds at 65°C in a water bath. Near the interface, a reddish-brown tint indicated the presence of terpenoids [87].

3.6 Characterization studies

To ensure the success of the synthetic process and determine whether the morphologies, particle size, functional group, and other properties required for the material to be used as an adsorbent are the synthesized PANI/magnetite (Fe3O4) adsorbent was characterized using a range of instrumental techniques. ATR-FTIR (Perkin Elmer Spectrum 65 model FTIR), P-XRD (XRD-7000, SHIMADZU Corporation, Japan), and UV-DRS (UV-Vis NIR CLB, Model V-770) were used to describe the synthesized sample.

3.7 Adsorption study of Rhodamine blue dye by biosynthesized PANI/magnetite adsorbent

3.71 Stock solution preparation

In this paper, adsorption tests were conducted using RB powder as the adsorbate molecule. The RB stock solution was made by dissolving 1 g of RB in 1000 mL of distilled water, which produced 1000 mg/L. The standard 1000 mg/L dye solution was used to create additional 1, 5, 10, and 15 mg/L working standard solutions of RB using the dilution rule [89].

3.7.2 Batch adsorption experiment

Each batch test was carried out at a constant 25 °C. Using 0.1 M NaOH and HCl, the design solutions pH was adjusted. The parameters that were chosen as independent variables were pH, sorbent dosage, contact time, and initial RB dye concentration. The output response was the removal efficacy of RB. Batch mode sorption was investigated for distinct parameters in a 250 mL conical flask. Various factors, including pH, adsorbent dosage, adsorb ate concentration, and contact time, are investigated by varying any one of them while keeping the others constant. To determine the impact of these variables on the change in removal capacity, adsorption kinetics and isotherms are investigated. For every measurement, samples were agitated, taken out of the flask at regular intervals, and filtered through Whitman filter paper. The following were the experimental variables' study ranges: starting concentrations (10, 15, 20, & 25 mg/L), contact duration (30, 50, 70, 90 & 110 minutes), adsorbent dosage (40, 60, 80, 100, 120 mg), and pH of solutions (2, 4, 6, 8, & 10).The absorbance of the filtrate solutions was determined by using a UV-visible Spectrophotometer at the maximum wavelength of 554 nm and it is possible to calculate the removal efficiency of PANI/Fe_3O_4 NCs by using Equation 5.

$$q_e = \frac{(Co - Ce)V}{W} \quad \ldots\ldots\ldots \quad (Eq5)$$

Where, qe is the equilibrium adsorption capacity per gram dry weight of adsorbents, mg/g: Co is the initial concentration of RB (mg L^{-1}), Ce, is the final concentration of RB (mg L^{-1}), V, is the volume of the solution (L), respectively.

The removal percentage was determined by using the following equation.

$$E = \frac{(Co - Ce)}{Co} * 100 \ldots\ldots\ldots\ldots\ldots\ldots\ldots\ldots\ldots\ldots\ldots\ldots\ldots\ldots\ldots\ldots\ldots\ldots\ldots\ldots\ldots\ldots\ldots\ldots\ldots\ldots\ldots (Eq6)$$

Where, Co and Ce represent the initial and final concentration (mg/l), respectively

3.8 Adsorption isotherm study

The suitability of the adsorption approach for the removal of RB from contaminated water was assessed by examining adsorption isotherms. Adsorbent-adsorb ate interactions are also described by several models for the adsorption isotherms. These models are based on several theories, chiefly on the kind of coverage, the interaction potential of the adsorbate species, and the homogeneity or heterogeneity of the adsorbents. The two equilibrium models that are used the most are Freundlich and Langmuir isotherms [90].

Adsorption isotherm studies were conducted to examine the connection between the concentration of the adsorbate in the solid phase and the solution phase at an equilibrium condition.

Langmuir isotherm determined by the following equation (7)

$$\frac{1}{\mathrm{qe}} = \frac{1}{KL\, qmax} * \frac{1}{Ce} + \frac{1}{qmax} \ldots\ldots\ldots\ldots\ldots\ldots\ldots\ldots\ldots\ldots\ldots\ldots\ldots\ldots\ldots\ldots\ldots\ldots\ldots\ldots\ldots (Eq7)$$

Freundlich isotherm determined under the following equation (8)

$$\ln \mathrm{qe} = \ln Kf + \frac{1}{n} * \ln Ce \ldots\ldots\ldots\ldots\ldots\ldots\ldots\ldots\ldots\ldots\ldots\ldots\ldots\ldots\ldots\ldots\ldots\ldots\ldots\ldots\ldots\ldots\ldots (Eq8)$$

3.9 Adsorption kinetics study

The most popular models for fitting kinetic sorption experiments to study the adsorption rate processes are pseudo-first-order and pseudo-second-order models. The solute uptake rate, which in turn controls the residence duration of the adsorption reaction, is described by the kinetics of adsorption [89]. It is among the crucial elements that determine the adsorption efficiency. Pseudo-first order kinetics as calculated by equation (9)

$$\ln(\mathrm{qe} - \mathrm{qt}) = lnqe - K1 * t \ldots\ldots\ldots\ldots\ldots\ldots\ldots\ldots\ldots\ldots\ldots\ldots\ldots\ldots\ldots\ldots\ldots\ldots\ldots\ldots (Eq9)$$

Pseudo-second order kinetics are determined by the following equation (10)

$$\frac{\mathrm{t}}{\mathrm{qt}} = \frac{1}{K2\ \mathrm{qe}^2} + \frac{1}{qe} * t \ldots\ldots\ldots\ldots\ldots\ldots\ldots\ldots\ldots\ldots\ldots\ldots\ldots\ldots\ldots\ldots\ldots\ldots\ldots\ldots\ldots\ldots\ldots\ldots . (Eq10)$$

CHAPTER FOUR

4 RESULT AND DISCUSSION

4.1 Phytochemical test results

The secondary metabolites present in *Croton macrostachyus* (Hoechst. Ex Delile) leaf extract, including alkaloids, flavonoids, carbohydrates, phenols, saponins, and tannins, play a critical role in the green synthesis of nanoparticles [72]. These compounds, particularly phenolic and tannin compounds, are well-known for their reducing capabilities, allowing them to effectively reduce metal salts like silver, zinc, and copper to their metallic nanoparticle forms. In this study, the presence of these phytochemicals in the *Croton macrostachyus* leaf extract made it an excellent candidate for use as both a reducing and stabilizing agent in the synthesis of PANI (polyaniline), Fe_3O_4 (magnetite) nanoparticles, and PANI/Fe_3O_4 adsorbent[73].

The results of the phytochemical screening confirmed that the leaf extract contains a variety of bioactive compounds, which have been shown to facilitate the reduction of metal ions, leading to the formation of nanoparticles. These secondary metabolites not only aid in the synthesis of nanoparticles but also help stabilize them, preventing aggregation and ensuring their uniform distribution in the composite material. This is in line with previous studies on Croton macrostachyus, which demonstrated similar findings, highlighting its potential for use in green nanotechnology applications. [87]

Moreover, the phytochemical composition of *Croton macrostachyus* extract aligns with the findings of other studies, such as one conducted on cinnamon bark extract. This study also identified the presence of tannins, saponins, phenols, and terpenoids, which exhibited similar reducing and stabilizing effects during nanoparticle synthesis. This comparison underscores the commonality of these secondary metabolites across different plant species and their utility in nanoparticle synthesis, as shown in Figure 1 and Table 1 of the study. These consistent results further validate the effectiveness of plant extracts, particularly those rich in polyphenolic compounds, in green synthesis methodologies for producing environmentally friendly and stable nanoparticle [91].

Figure 1: Phytochemical test result of *Croton macrostachyus* extract for (a) coumarins (b) tannins(c) glycoside, (d) flavonoid, (e) phenolic, (f) saponins, (g) steroid and (h) terpenoids, plant constituent metabolites [91].

Table 1: Phytochemical Screening of *Croton macrostachyus* Leaf Extracts

No	Chemical constituent	Results
1	Test of coumarins (Alkaline reagent test)	+
2	Test of Tannins	+++
3	Test of Glycosides	++
4	Test of Flavonoids	+
5	Test of Phenol	++
6	Test of Saponins	+
7	Test of Steroids	+
8	Test of Terpenoids	+

Note: +++ most present, ++ more present, + moderate [91].

The results of the phytochemical screening of *Croton macrostachyus* aqueous leaf extract, as presented in Table 1, provide important insights into the presence and concentration of various bioactive compounds that contribute to its potential as a reducing and stabilizing agent in nanoparticle synthesis. The table categorizes the results based on the intensity of presence, using a scale of “+”, “++”, and “+++”, indicating moderate, more present, and most present levels of each chemical constituent, respectively. These compounds, which include tannins, flavonoids, phenols, saponins, and others, play crucial roles in the reduction of metal ions and stabilization of nanoparticles during synthesis.

Presence of Tannins and Glycosides

Tannins, which are listed as "+++," are the most prominent secondary metabolites identified in the *Croton macrostachyus* leaf extract. Tannins are well-known for their strong reducing ability and are commonly used in the green synthesis of nanoparticles due to their ability to stabilize the resulting particles by preventing aggregation. In the context of nanoparticle synthesis, tannins can chelate metal ions and facilitate their reduction to metallic nanoparticles. Glycosides, also present in moderate abundance (“++”), are another important class of compounds that could potentially contribute to the synthesis of nanoparticles. These compounds are known for their various biological activities, and although they are not typically as strongly reducing as tannins, they may still play a supportive role in the reduction process.

Flavonoids and Phenols: Moderate but Important

Flavonoids and phenols are also present in the leaf extract, albeit at lower levels ("+" for flavonoids and "++" for phenols). Flavonoids are known for their antioxidant properties, and their presence in the extract could contribute to the stabilization of nanoparticles by preventing oxidative degradation. Phenolic compounds, being strong reducing agents, are often involved in the reduction of metal salts to nanoparticles. Although present in moderate concentrations, both flavonoids and phenols are likely to enhance the overall reducing and stabilizing effects in the synthesis process. The combination of these compounds with the higher concentrations of tannins creates a synergy that enhances the overall efficacy of the leaf extract in nanoparticle formation.

Other Compounds: Saponins, Coumarins, Steroids, and Terpenoids

Other notable compounds identified in the *Croton macrostachyus* leaf extract include saponins, coumarins, steroids, and terpenoids. Saponins, though present in lower concentrations ("+"), are known for their surfactant properties, which could help in stabilizing nanoparticles by preventing

agglomeration. Coumarins, although less abundant ("+"), have been shown to possess antimicrobial and antioxidant properties, which could further benefit the nanocomposite's overall stability and functionality. Steroids and terpenoids, both identified in small quantities ("+"), are less commonly associated with nanoparticle synthesis, but they may contribute additional bioactive properties to the nanocomposites, such as enhancing the overall biological activity or contributing to the material's stability. The presence of these compounds enriches the phytochemical profile of the *Croton macrostachyus* leaf extract, making it a versatile source for the green synthesis of PANI/Fe_3O_4 adsorbent.

In summary, the phytochemical screening of *Croton macrostachyus* leaf extract reveals a rich array of bioactive compounds that contribute to its efficacy in nanoparticle synthesis. The dominant presence of tannins and phenols, along with the supportive roles of flavonoids, saponins, and other secondary metabolites, highlights the extract's potential as an environmentally friendly and effective reducing and stabilizing agent in the creation of functional nanomaterials like PANI/Fe_3O_4 adsorbent.

4.2 Characterization of synthesized adsorbent

4.2.1 UV-Vis DRS Analysis

The UV-vis diffuse reflectance spectroscopy (UV-vis-DRS) technique was employed to analyze the spectra of the resulting PANI/Fe_3O_4 adsorbent, which were dispersed in water. The aim was to identify the characteristic absorption bands associated with the individual components of the adsorbent. The analysis revealed that the pure PANI exhibited a characteristic absorption peak around 340 nm, which corresponds to the π-π^* transition of the polymers conjugated system. On the other hand, Fe_3O_4 nanoparticles displayed an absorption peak at 365 nm, which is typical for magnetite nanoparticles due to their electronic structure [92].

For the PANI/Fe_3O_4 adsorbent, a significant shift in the absorption spectrum was observed, with a broad peak appearing in the range of 700-800 nm. This peak is associated with the π-polaron transition, a feature indicative of the conduction band in conducting polymers like PANI. The appearance of this new absorption band in the PANI/Fe_3O_4 adsorbent and the PANI/Fe_3O_4 adsorbent spectrum at a higher wavelength (700-800 nm) is a direct result of the interaction between the PANI and Fe_3O_4 nanoparticles. The shift to this higher wavelength (725 nm) suggests that the increased concentration of Fe_3O_4 in the adsorbent enhances the coupling between the PANI

matrix and the magnetite nanoparticles. This structure of PANI, causing the π-polaron transition to occur at a longer wavelength, which is consistent with previous studies on similar PANI/Fe_3O_4 adsorbent [92].Furthermore, the increase in the Fe_3O_4 content in the PANI matrix led to a stronger and more pronounced absorption peak at this higher wavelength, further supporting the idea of significant interaction between the polymer and nanoparticles. These spectral changes indicate that the Fe_3O_4 nanoparticles are not simply dispersed within the PANI matrix but are interacting at the molecular level, likely influencing the electronic properties of PANI and contributing to the overall stability and functionality of the adsorbent. This behavior is essential for applications that rely on the electrical or magnetic properties of such hybrid materials, as the interaction between the components can significantly impact their performance.

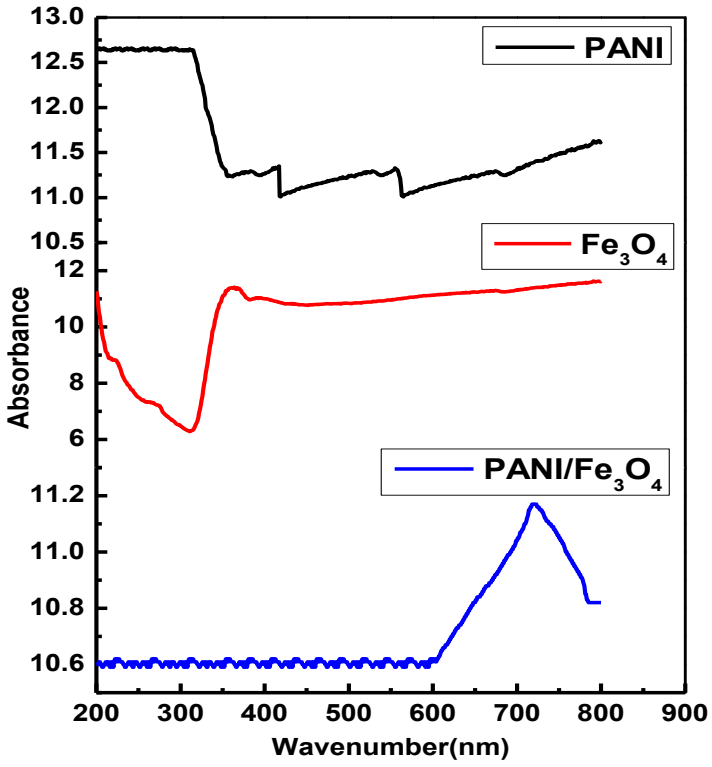

Figure 2: UV-Vis DRS spectrum of PANI, Fe3O4, and PANI/Fe3O4 adsorbent

4.2.2 X-ray Diffraction analysis (P-XRD)

The phase purity and crystallinity of the synthesized magnetite nanoparticles (Fe_3O_4 NPs), polyaniline (PANI), and PANI/Fe_3O_4 adsorbent were evaluated through X-ray diffraction (XRD) analysis, a powerful technique used to study the crystalline structure of materials. The XRD pattern of the synthesized magnetite sample revealed six distinct peaks, corresponding to specific diffraction angles (2θ), as shown in Figure 3. These peaks appeared at 2θ values of 30.40°, 35.42°, 43.34°, 53.82°, 57.18°, and 62.40°, which correspond to the crystal planes (220), (311), (400), (422), (511), and (440) of magnetite (Fe_3O_4).The presence of these well-defined peaks indicates that the magnetite nanoparticles possess high crystallinity and phase purity. These diffraction peaks match closely with the standard reference data from the Joint Committee on Powder Diffraction Standards (JCPDS) card number 00-019-0629, which confirms that the synthesized Fe_3O_4 nanoparticles are indeed magnetite and do not contain any secondary phases or impurities. The absence of additional peaks suggests that no unwanted phases were formed during the synthesis process, thus ensuring the purity of the magnetite nanoparticles. This XRD data is crucial for confirming the successful synthesis of magnetite nanoparticles and provides strong evidence of their crystallinity. In the context of the PANI/Fe_3O_4 adsorbent, XRD analysis also helps in understanding the structural integrity of the adsorbent material. Any shifts in peak positions or changes in peak intensities when comparing pure Fe_3O_4 to the nanocomposites could indicate interactions between the PANI matrix and the Fe_3O_4 nanoparticles, which would affect the overall crystalline structure and phase behavior of the composite. Thus, the XRD results not only confirm the quality of the Fe_3O_4 nanoparticles but also lay the foundation for understanding the structural properties of the PANI/Fe_3O_4 adsorbent in subsequent analyses [93].The X-ray diffraction (XRD) analysis of the PANI/Fe_3O_4 adsorbent reveals a distinct structural pattern with specific diffraction peaks that correspond to both the Fe_3O_4 nanoparticles and the polyaniline (PANI) polymer matrix. The XRD pattern of the PANI/Fe_3O_4 nanocomposites displays peaks at 2θ values of 11.30°, 27.34°, 32.40°, 35.42°, 61.28°, 63.08°, and 68.20°, which correspond to the crystal planes (101), (110), (220), (311), (422), (440), and (511), respectively. These values are consistent with the diffraction patterns of magnetite (Fe_3O_4), confirming that the magnetite nanoparticles are present in the composite and maintain their crystalline structure.

The obtained XRD results also show a broad peak in the range of 2θ = 20-30°, which is characteristic of amorphous materials [94]. This broad diffraction peak can be attributed to the PANI component in the nanocomposite. The specific diffraction peak centered at 2θ = 25.32° is identified as the characteristic peak of PANI, corresponding to the (101) crystal plane. This peak is indicative of the periodicity and ordered arrangement of the polymer chains, with the periodicity parallel and perpendicular to the PANI chains. The broadness of the PANI peak suggests that the polymer itself is relatively amorphous, which is typical for PANI in its emeraldine form, where the polymer chains lack long-range crystalline order. Importantly, no additional peaks corresponding to other phases or impurities were observed in the XRD pattern, which confirms that the PANI/Fe_3O_4 adsorbent is pure and free from secondary phases. The pattern reveals only the characteristic peaks of Fe_3O_4 and PANI, suggesting that the formation of the nanocomposite did not lead to the generation of unwanted byproducts. However, the intensity and position of the Fe_3O_4 peaks in the composite show slight changes compared to pure Fe_3O_4 nanoparticles. These subtle shifts in peak intensity and position may be attributed to the interaction between the PANI matrix and the Fe_3O_4 nanoparticles, potentially forming a heterojunction interface at the PANI-Fe_3O_4 interface. This heterojunction can influence the electronic properties of the adsorbent, enhancing its functionality for applications such as sensors, catalysis, and environmental remediation. Generally, the XRD analysis demonstrates that the PANI/Fe_3O_4 adsorbent retains the characteristic crystalline structure of magnetite while incorporating PANI in an amorphous form. The changes in the Fe_3O_4 peak intensities and positions suggest strong interactions between the polymer and the nanoparticles, which may play a crucial role in the composite's properties. The absence of additional peaks indicates the successful synthesis of a pure composite material, highlighting the effectiveness of the sol-gel method in creating a well-formed PANI/Fe_3O_4 adsorbent.

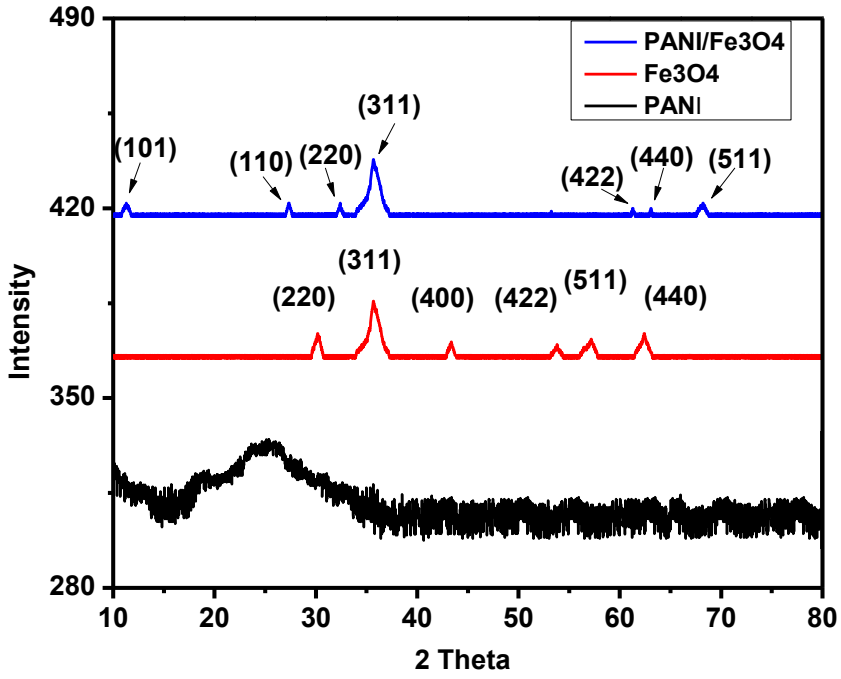

Figure 3 : XRD patterns of PANI, Fe3O4 NPs and PANI/Fe3O4 adsorbent

.

The crystalline size of the PANI/Fe_3O_4 adsorbent was estimated using Scherer's equation, which is commonly applied to calculate the average size of crystalline nanoparticles from the broadening of XRD peaks. Scherer's equation is given by:

$$D = \frac{k\lambda}{\beta cos\theta} \quad \text{(Eq11)}$$

Where:

D is the crystalline size (in Å or nm), k is the shape factor (typically 0.89 if the shape is unknown), λ is the wavelength of the X-ray (0.154 nm), β is the full width at half maximum (FWHM) of the XRD peak (in radians), θ is the Bragg's angle (in degrees). In this study, the broad diffraction peak at $2\theta = 35.42°$ was selected for the calculation because it is one of the significant peaks corresponding to the Fe_3O_4 crystal planes (311), which are well-defined in the XRD pattern. By applying Scherer's equation, the crystalline size of the PANI/Fe_3O_4 adsorbent was estimated to be 14 nm.

This crystalline size is in line with the typical range of nanoparticle sizes observed for Fe_3O_4 nanoparticles and suggests that the PANI/Fe_3O_4 adsorbent has a relatively small average crystallite size. The small particle size is advantageous for various applications, including environmental remediation and catalysis, as it provides a large surface area for interaction with contaminants or reactants. Additionally, the fact that the size of the composite is similar to that of pure Fe_3O_4 nanoparticles indicates that the incorporation of PANI into the composite does not significantly alter the crystallinity or particle size of Fe_3O_4 but may influence other properties such as electronic conductivity, adsorption capacity, and stability.

Overall, the XRD analysis and the use of Scherer's equation provide valuable insights into the crystalline structure and size of the PANI/Fe_3O_4 adsorbent, reinforcing the idea that these nanocomposites maintain the desirable properties of the individual components while offering enhanced functionality due to their hybrid nature.

4.2.3 FT-IR (Fourier-transform infrared) spectroscopy

To understand the molecular structure of the PANI/Fe_3O_4 adsorbent, FT-IR (Fourier-transform infrared) spectroscopy was performed on pure PANI, Fe_3O_4, the PANI/Fe_3O_4 adsorbent , and the plant extract used for synthesis. The FT-IR spectra, shown in Figure 4, provide detailed insights into the functional groups and bonding present in the materials.

The FT-IR spectrum of pure PANI (black line in Figure 7) shows characteristic absorption peaks. The peaks at 1,572 cm^{-1} and 1,500 cm^{-1} correspond to the stretching modes of the N=Quinone (Q) =N ring and the N-benzene (B)-N ring, respectively, reflecting the conjugated structure of the PANI polymer. The peak at 1,380 cm^{-1} is attributed to the C–N (aromatic–N) deformation, which is a signature of the aromatic nature of PANI [95]. A distinct peak at 1,135 cm^{-1} is associated with the C–N stretching vibrations, further supporting the presence of the polymer backbone. The peak at 1,182 cm^{-1} corresponds to the B–NH vibration mode, and the peaks between 900–700 cm^{-1} are characteristic of the aromatic ring's out-of-plane C–H deformation vibrations, which are common in aromatic polymers like PANI.

For the green-synthesized magnetite nanoparticles (red line in Figure 4), the FT-IR spectrum reveals several important peaks. The broad absorption band at 3,225 cm^{-1} indicates the O-H stretching vibration, which is typically associated with alcohols or phenolic compounds. This suggests the presence of hydroxyl groups in the magnetite structure or adsorbed water molecules. The band at 1,569 cm^{-1} is related to the C=C stretching vibration, which can be assigned to the

carbonyl group of the plant extract components that may be interacting with the magnetite. The peaks at 1,343 cm^{-1} and 1,071 cm^{-1} are likely associated with C–O stretching vibrations, indicative of alcohol or phenolic groups in the plant extract [96].

In addition to these organic functional groups, the magnetite nanoparticles show two important peaks at 550 cm^{-1} and 432 cm^{-1}, which are characteristic of Fe–O stretching vibrations in the spinel-type structure of magnetite (Fe_3O_4). These peaks confirm the presence of the Fe_3O_4 phase in the synthesized nanoparticles and indicate the successful formation of magnetite. The two distinct absorption bands at these lower wavenumbers reflect the octahedral and tetrahedral sites in the Fe_3O_4 crystal structure, further confirming the phase purity of the magnetite nanoparticles.

The FT-IR analysis of the PANI/Fe_3O_4 adsorbent provides valuable information about the molecular interactions and functional groups present in the material. The FT-IR spectra reveal the characteristic features of both PANI and Fe_3O_4, confirming the successful incorporation of magnetite nanoparticles into the PANI matrix and providing evidence for the interactions between the polymer and the nanoparticles. Additionally, the presence of functional groups from the plant extract further supports its role in the green synthesis process, acting as both a reducing and stabilizing agent for the nanoparticles.

The FT-IR analysis provided valuable insights into the molecular structures of the PANI/Fe_3O_4 adsorbent, revealing the characteristic functional groups of both PANI and Fe_3O_4, as well as the influence of Fe_3O_4 nanoparticles on the PANI matrix. In Figure 4 (blue line graph), the FT-IR spectra of PANI containing varying levels of Fe_3O_4 nanoparticles show key absorption peaks that correspond to the individual components and their interactions.

For the Fe_3O_4 nanoparticles, the peaks at 432 cm^{-1} and 550 cm^{-1} are attributed to the Fe-O stretching vibrations, which are characteristic of the magnetite structure. These peaks confirm the presence of Fe_3O_4 in the nanocomposite. When Fe_3O_4 nanoparticles are incorporated into the PANI matrix, several distinct peaks associated with PANI are observed, including the 3320 cm^{-1} peak (N-H stretching), which is typical of the primary amine group present in PANI. The peaks at 1520 cm^{-1} and 1548 cm^{-1} correspond to C=C stretching vibrations, which are indicative of the benzenoid and quinoid rings in the PANI structure [97]. These bands reflect the conjugated nature of the polymer chain. Another important feature is the peak at 1310 cm^{-1}, which represents the C–N stretching vibration of the aromatic secondary amine group in PANI. Additionally, the peaks at 1120 cm^{-1} and in the range of 900–800 cm^{-1} are associated with out-of-plane deformation

vibrations of the C–N bonds in the 1, 4-distributed benzene rings of PANI. These peaks confirm that the PANI structure is well preserved in the composite, and that Fe_3O_4 nanoparticles are successfully incorporated.

Interestingly, the blending of Fe_3O_4 nanoparticles with PANI causes shifts in several IR bands, which suggests that the nanoparticles interact with the polymer matrix. These shifts can be attributed to the formation of hydrogen bonds (H-bonds) between the protons within the N-H group of PANI and the oxygen atoms on the surface of Fe_3O_4 nanoparticles [98]. Such interactions might contribute to enhanced stability and stronger bonding within the nanocomposite, which could influence its properties, such as its adsorption capacity, conductivity, or catalytic activity.

In addition to the PANI/Fe_3O_4 adsorbent, the FT-IR spectrum of the Croton macrostachyus leaf extract (green line in Figure 4) was also analyzed to understand the role of the plant extract in the synthesis process. The FT-IR spectrum of the leaf extract reveals several important functional groups that may be involved in the green synthesis of Fe_3O_4 nanoparticles. The broad peak at 3315 cm^{-1} is characteristic of the O-H stretch from alcohols, while the peak at 2980 cm^{-1} corresponds to the C-H stretch of alkanes. Additional peaks at 2440 cm^{-1} and 2145 cm^{-1} confirm the presence of C≡C stretching, indicative of alkynes. The band at 1642 cm^{-1} is attributed to the stretching vibration of the aldehyde carbonyl (C=O) group, which is likely associated with cinnamaldehyde, a major component in the plant extract. Other significant peaks include 647 cm^{-1} (vibration of alkanes), 751 cm^{-1} (benzene rings =CH), 1059 cm^{-1} (C–O stretching), 1342 cm^{-1} (C–N stretching of aromatic amines), and 1488 cm^{-1} (C=C bonds) [97]. These peaks suggest that the plant extract contains a variety of polyphenolic and flavonoid compounds, such as cinnamaldehyde, which are known to have reducing and stabilizing properties. These compounds likely play a crucial role in the green synthesis process, reducing metal ions and stabilizing the Fe_3O_4 nanoparticles.

The FT-IR spectra provide detailed information about the molecular structure and functional groups present in the PANI/Fe_3O_4 adsorbent. The characteristic peaks of both PANI and Fe_3O_4 confirm their successful incorporation into the nanocomposite, while the shifts in the IR bands indicate interactions between the two components. Additionally, the FT-IR spectrum of the plant extract highlights the role of secondary metabolites, such as phenols, flavonoids, and aldehydes, in the green synthesis of Fe_3O_4 nanoparticles and their interaction with the polymer matrix. This molecular-level understanding of the PANI/Fe_3O_4 adsorbent can help in tailoring their properties for specific applications, such as adsorption, catalysis, and environmental remediation.

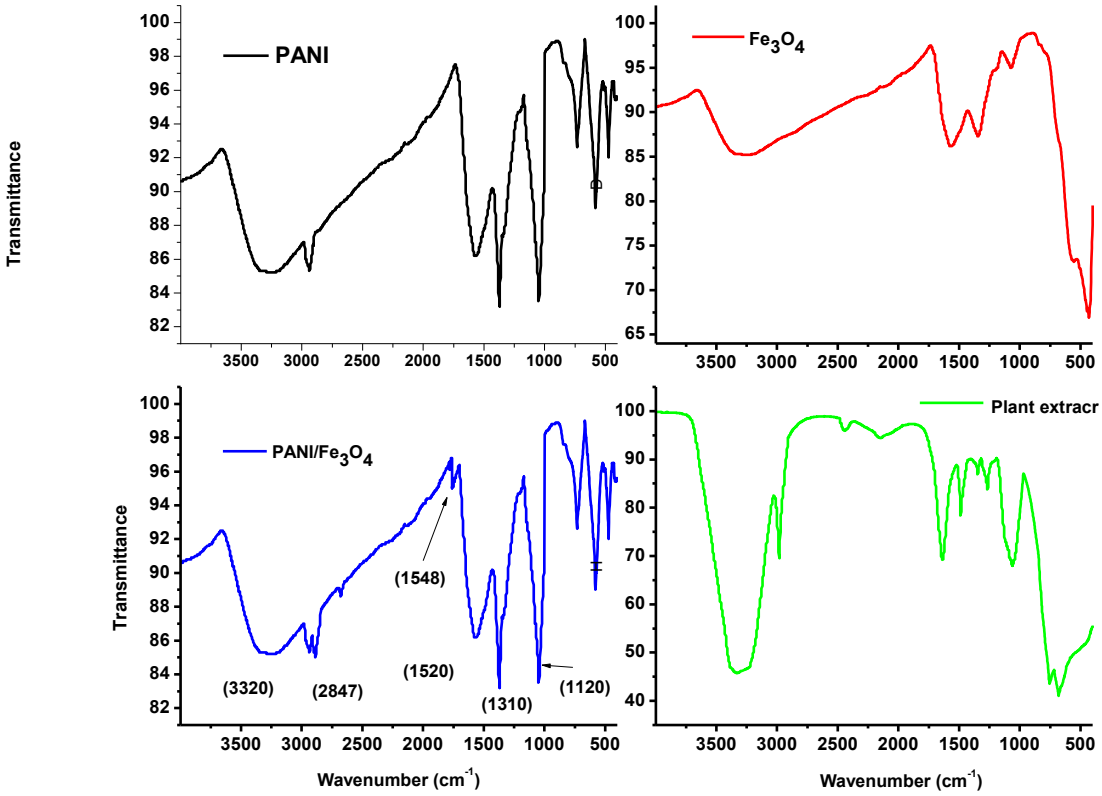

Figure 4: FTIR spectrum data of Plant extract, PANI, Fe_3O_4 NPs, and PANI/Fe_3O_4 adsorbent.

4.3 Optimization of adsorbent for removal efficiency of rhodamine blue dye from aqueous solution

4.3.1 Calibration plot of working rhodamine blue standard solution

The calibration plot for Rhodamine B (RhB) dye at 554 nm was used to quantify the residual concentration of the dye in the filtrate after adsorption using the synthesized adsorbents, including PANI, magnetite (Fe_3O_4), and PANI/Fe_3O_4 adsorbent. The absorbance of RhB at this wavelength is directly proportional to its concentration in solution, allowing for the determination of the dye concentration before and after adsorption.

The data from the calibration plot, shown in Figure 5, provide a clear relationship between the absorbance at 554 nm and the concentration of RhB dye in the solution. As RhB dye was adsorbed onto the surface of the adsorbents, the concentration of the dye in the filtrate decreased, leading to a reduction in absorbance at 554 nm. This decrease in absorbance corresponds to the amount of RhB dye removed from the aqueous solution by the adsorbent.

Table 2 presents the specific concentrations of RhB dye remaining in the solution after treatment with each adsorbent at different time intervals, based on the calibration curve. These results are essential for evaluating the adsorption efficiency of the synthesized adsorbents. By comparing the initial concentration of RhB dye with the final concentration in the filtrate, the adsorption capacity of PANI, Fe_3O_4, and PANI/Fe_3O_4 adsorbent can be calculated, and their relative efficiencies in dye removal can be assessed.

The calibration plot and the associated data provide a reliable method for assessing the adsorption performance of the nanocomposites, offering insights into their potential applications in wastewater treatment, particularly for the removal of organic dyes such as RhB. The analysis of these results also allows for a detailed comparison between the different adsorbents, shedding light on the impact of Fe_3O_4 incorporation into PANI on the adsorption efficiency.

Table 2: Rhodamine blue dye working standard solution calibration data

The initial concentration of RhB(mg/L)	Absorbance
10	1.464
15	2.178
20	2.835
25	3.584

The calibration data for Rhodamine Blue (RhB) dye working standard solution provides important insights into the relationship between the concentration of the dye and its absorbance at a specific wavelength (typically 554 nm). In this analysis, we can observe a clear linear trend between the initial concentration of RhB dye (in mg/L) and the measured absorbance. The Rhodamine Blue (RhB) dye calibration data shows a consistent and linear relationship between the initial concentration of RhB and the measured absorbance at 554 nm. This linearity supports the use of the calibration plot for quantifying the concentration of RhB dye in solution, making it an effective tool for evaluating the efficiency of adsorbents in removing RhB dye during wastewater treatment processes. The data suggests that RhB dye follows Beer-Lambert's Law in the concentration range provided, allowing for accurate determination of dye removal in experimental studies

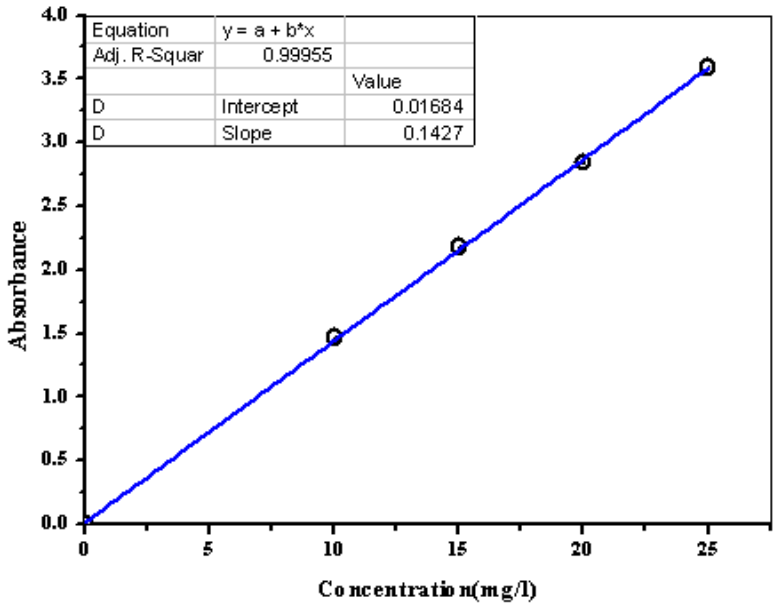

Figure5: Calibration plot of working rhodamine blue standards solution

4.4 RhB dye adsorption by using PANI, Fe_3O_4 NPs, and PANI/Fe_3O_4 NPs adsorbent

4.4.1 Effect of pH

The pH of the dye solution plays a crucial role in the adsorption process, as it influences the surface charge of the adsorbents as well as the ionization state of the dye molecules. In the present study, the effect of pH on the adsorption of Rhodamine Blue (RhB) dye was investigated by adjusting the pH of the solution between 2 to 10 and adding 80 mg of PANI, Fe_3O_4, and PANI/Fe_3O_4 adsorbent to 10 mg/L RhB solution for a contact time of 50 minutes. The results showed a significant increase in dye uptake with increasing pH, as depicted in Figure 5, highlighting the importance of pH in optimizing the adsorption process.

At low pH (pH 2), the adsorption efficiency of the cationic dye RhB is lower for all three adsorbents (PANI, Fe_3O_4, and PANI/Fe_3O_4), as the surface of the adsorbents is more likely to be protonated. This reduces the electrostatic interaction between the adsorbent and the cationic dye, hindering the adsorption process. This behavior is consistent with the general principle that cationic dyes like RhB adsorb poorly at pH values Lowe. Where the adsorbent surface becomes positively charged and repels the positively charged dye molecules [99].

However, as the pH increases the surface charge of the adsorbents shifts, becoming more negatively charged. This enhances the electrostatic attraction between the negatively charged adsorbent surface and the positively charged RhB molecules, leading to increased adsorption. In the current study, the adsorption of RhB dye was found to improve significantly as the pH increased, with the removal efficiencies rising from 86.04% at pH 2 to 91.22% at pH 10 for PANI, from 94.31% at pH 2 to 96.97% at pH 10 for Fe_3O_4 nanoparticles, and from 97.39% at pH 2 to 99.91% at pH 10 for the PANI/Fe_3O_4 adsorbent.

These results indicate that pH 10 is the optimal pH for dye removal using all three adsorbents. The PANI/Fe_3O_4 adsorbent exhibited the highest efficiency, with a 99.91% removal of RhB at pH 10, outperforming both the pure PANI and Fe_3O_4 adsorbent. This suggests that the incorporation of Fe_3O_4 nanoparticles into the PANI matrix enhances the adsorption capacity, likely due to the synergistic effect between the two components, which improves the interaction with the dye molecules.

Overall, the study underscores the importance of pH in the adsorption of cationic dyes like RhB. The PANI/Fe_3O_4 adsorbent proved to be the most efficient adsorbent at higher pH, making it a promising material for dye removal from wastewater in conditions where the pH is more alkaline.

In contrast, pure PANI and Fe_3O_4 adsorbent were less effective, with their adsorption capacities improving but still not reaching the performance of the PANI/Fe_3O_4 adsorbent at pH 10. Therefore, the optimal pH for the adsorption process of RhB dye using these adsorbents is pH 10, with PANI/Fe_3O_4 adsorbent being the most effective material for this application.

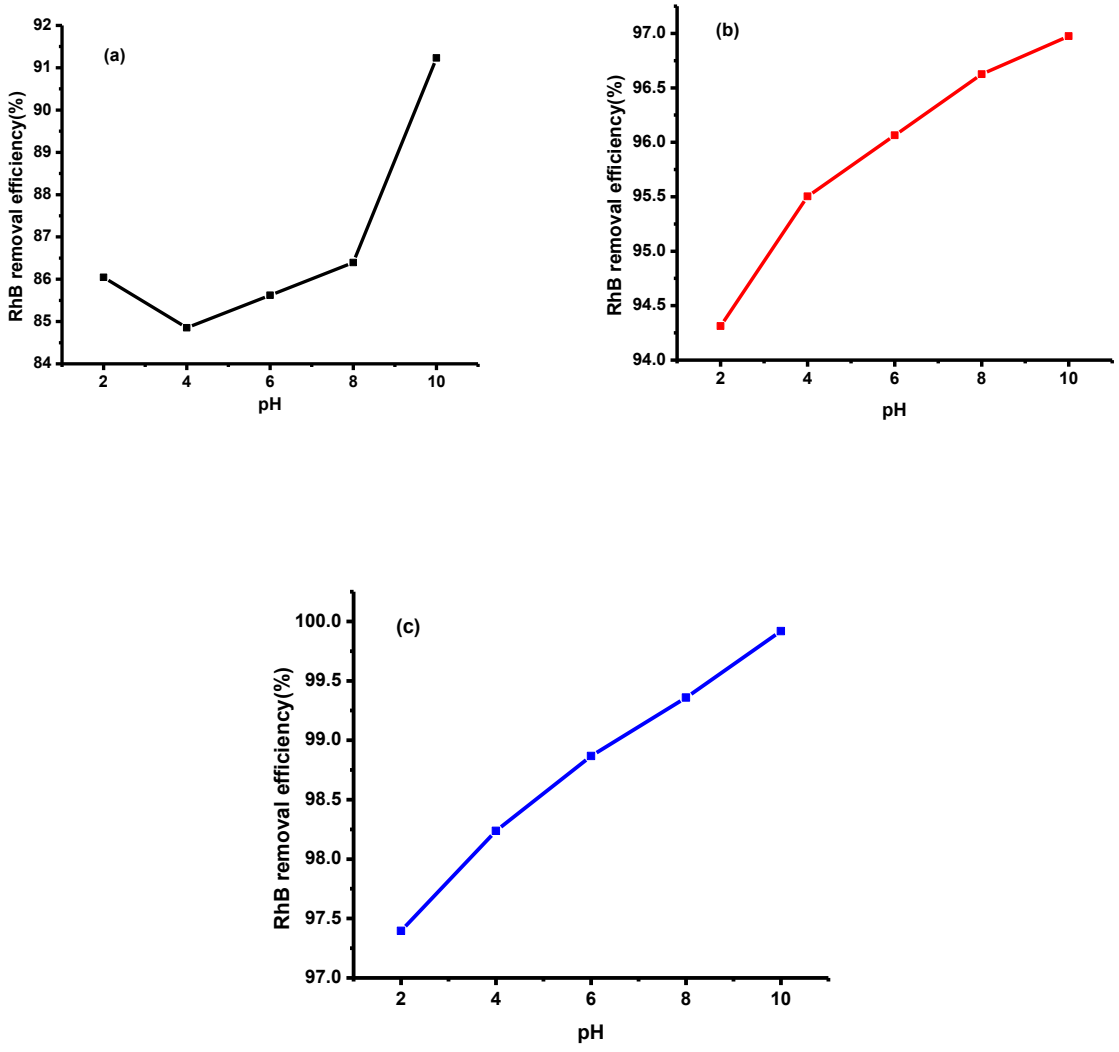

Figure 6: Effect of pH on RhB dye removal by (a) PANI, (b) Fe3O4 NPs, and (c) PANI/ Fe3O4 adsorbent at 80 mg adsorbent dose, 10 mg/L initial concentration, 50 minute contact time

4.4.2 Effect of adsorbent dosage

The adsorbent dosage is a key factor influencing the efficiency of dye removal during adsorption processes. In this study, the effect of varying adsorbent dosages of PANI, Fe_3O_4 and PANI/Fe_3O_4 adsorbent was evaluated at pH 10 with a contact time of 50 minutes and an initial RhB dye concentration of 10 mg/L. The adsorbent doses tested ranged from 40 to 120 mg for each of the three adsorbents. The results, shown in Figure 6 (a), (b), and (c), reveal how the adsorption efficiency of the adsorbents changes as the dosage increases.

For all three adsorbents, there was a clear trend: as the adsorbent dosage increased from 40 mg to 80 mg, the percentage removal of RhB dye improved significantly. Specifically, the dye removal efficiency increased to 91.22% for PANI, 96.97% for Fe_3O_4 NPs, and 99.91% for PANI/Fe_3O_4 nanocomposite. This increase in efficiency can be attributed to the availability of more adsorption sites as the dosage of the adsorbents increases. More adsorbent material provides a larger surface area for the dye molecules to interact with, which enhances the overall adsorption capacity and leads to better removal of RhB dye from the solution [100].

However, after 80 mg of adsorbent was used, further increases in the adsorbent dosage did not significantly improve the dye removal efficiency. At dosages higher than 80 mg, the adsorption effectiveness plateaued or even slightly declined. This behavior can be explained by adsorbent aggregation at higher doses, where the adsorbent particles tend to cluster together. Such aggregation reduces the number of available adsorption sites on the particle surface and can also limit the availability of dye molecules for adsorption. Additionally, when the adsorbent concentration is too high, there may not be enough dye molecules in the solution to fully occupy all of the available sites on the adsorbent, leading to wasted adsorbent and no significant increase in removal efficiency.

Based on these observations, the optimum adsorbent dosage was determined to be 80 mg for all three materials, as it provided the highest dye removal efficiency without any further significant improvements with higher dosages. This optimal dosage was then used for the subsequent experimental analyses. The results emphasize the importance of optimizing adsorbent dosage in order to achieve efficient dye removal while avoiding unnecessary use of material and minimizing cost in practical applications.

The findings suggest that PANI/Fe_3O_4 adsorbent is the most effective adsorbent for RhB dye removal, with an optimum dosage of 80 mg offering the highest removal efficiency of 99.91%.

This optimal dosage should be considered for further studies and potential applications in environmental remediation and wastewater treatment processes.

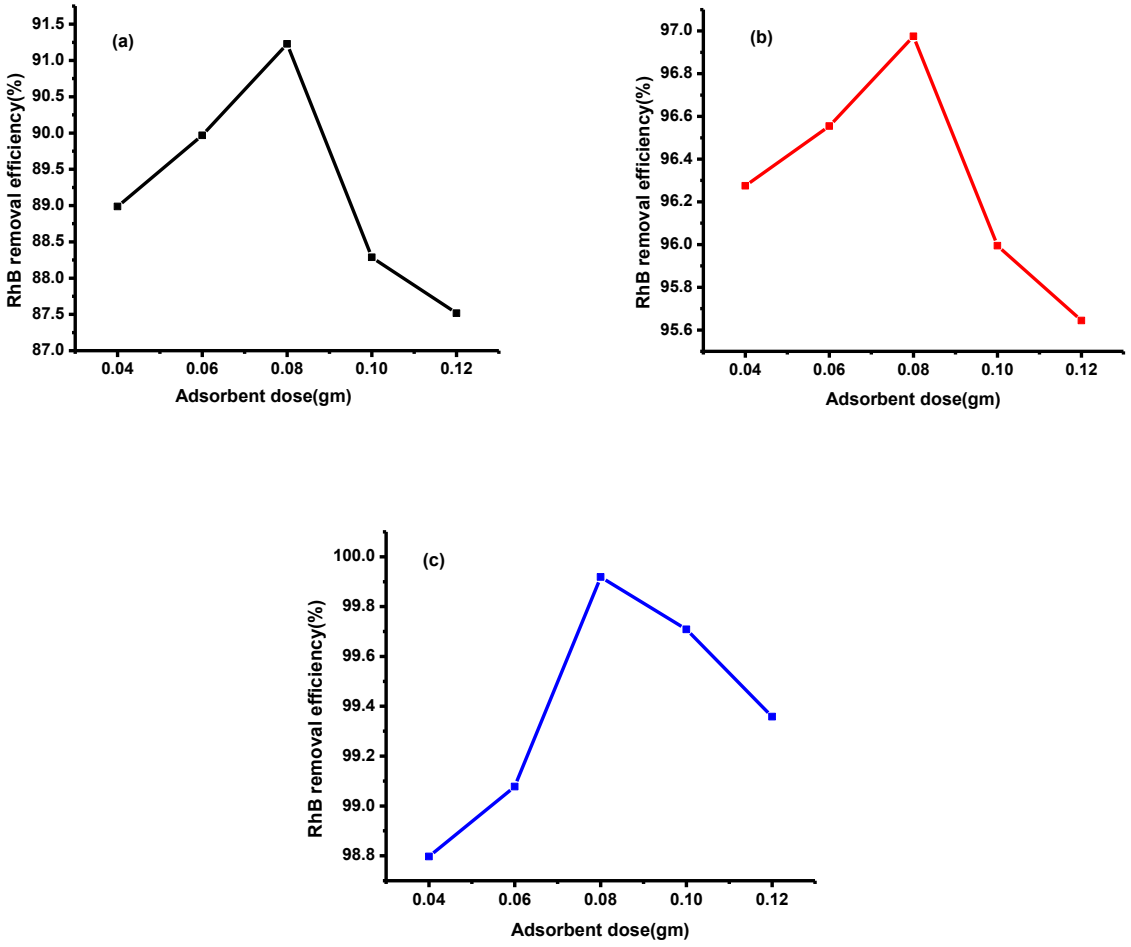

Figure 7: Effect of adsorbent dose on the removal of RhB dye by (a) PANI, (b) Fe3O4 and (c) PANI/Fe3O4 adsorbent at pH 10, 10 mg/L initial concentration, and 50 min contact time

4.4.3 Effect of contact time

As shown in Figures 7, (a), (b), and (c), the adsorption of rhodamine blue dye at an initial concentration of 10 mg/L was studied at different contact times (30–110 min) with an adsorbent dose of 80 mg, at pH 10 for three synthesized adsorbents, PANI, Fe_3O_4 NPs and PANI/Fe_3O_4 adsorbent. The data indicated that it takes only 50 minutes to reach equilibrium conditions. The high adsorption rate in the early contact times is caused by multiple activated adsorption sites that are available for dye molecules, increasing dye penetration to the adsorption surface. As the

adsorbent surface becomes saturated, the concentration gradient decreases over time, and the removal percentage roughly stays constant.

The dye removal percentage was 88.28% to 91.22% for PANI, 96.41% to 96.97% for Fe_3O_4 NPs, and 98.86% to 99.91% for the PANI/Fe_3O_4 adsorbent from the first 30 minutes to the equilibrium time of 50 minutes of adsorption. The adsorption increases with time and reaches equilibrium at 50 minutes with an adsorption efficiency of 99.91% for the nanocomposite adsorbent. This is because there are a large number of free adsorption sites during the initial stage of reaction, which decreases as the time increases and ultimately reaches equilibrium [101].

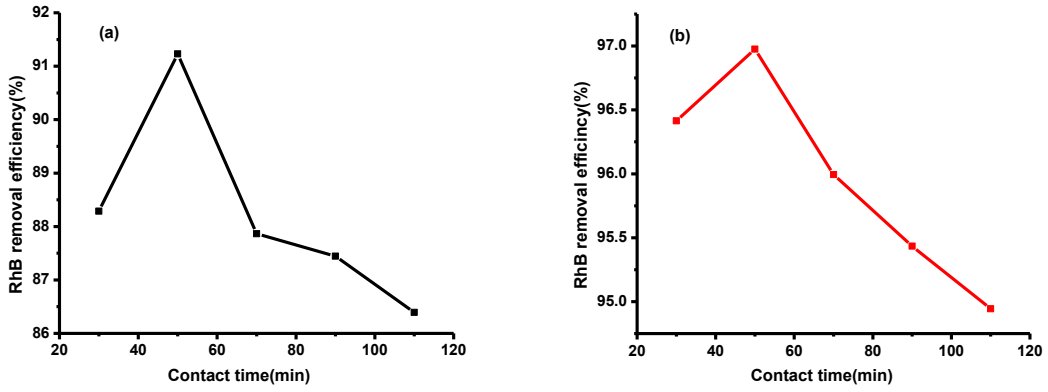

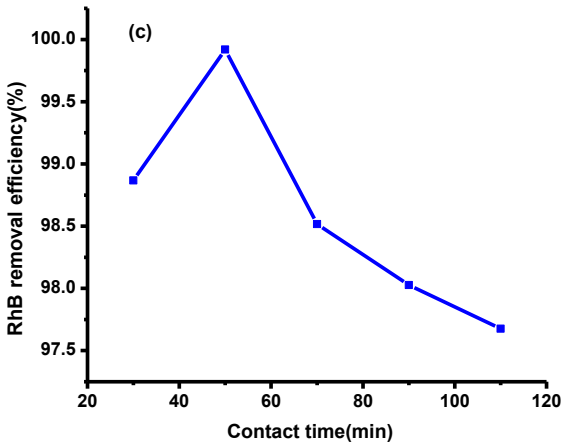

Figure 8: Effect of contact time on the removal of RhB dye by (a) PANI, (b) Fe3O4 NPs, and (c) PANI/Fe3O4 adsorbent at pH 10, 80mg dose and 10 mg/L initial concentration.

4.4.4 Effect of initial concentration

A series of experiments were carried out using varying concentrations of RhB dye solution (10, 15, 20, and 25 mg/L) with an 80 mg adsorbent dose of PANI, Fe_3O_4 NPs, and PANI/Fe_3O_4 adsorbent at pH 10, within 50 minutes of contact time in order to examine the impact of initial dye concentration on adsorption properties. At a lower initial concentration of RhB solution, the adsorption is quite rapid, as illustrated in Figure 8. Despite an increase in the amount of total RhB buildup, the result indicates that clearance efficiency reduced as initial concentrations increased. Based on the identical operating circumstances indicated in Figure below (a), (b), (c), it was found that utilizing PANI, Fe_3O_4 and PANI/Fe_3O_4 adsorbents, respectively, removed approximately 91.22%, 96.97%, and 99.91% of RhB at an initial concentration of 10 mg/L. It is possible that the saturation of adsorption sites on the adsorbent surface is the reason why the percentage of RhB removal falls as the starting dye concentration rises. At a low initial concentration, there are unoccupied active sites on the adsorbent surface, so most of the RhB solution might contact the active sites of adsorbents. However, at a higher concentration, most of the dye was not able to contact the active surfaces because the active sites might have been occupied by the RhB solution, which is consistent with the results obtained [102].

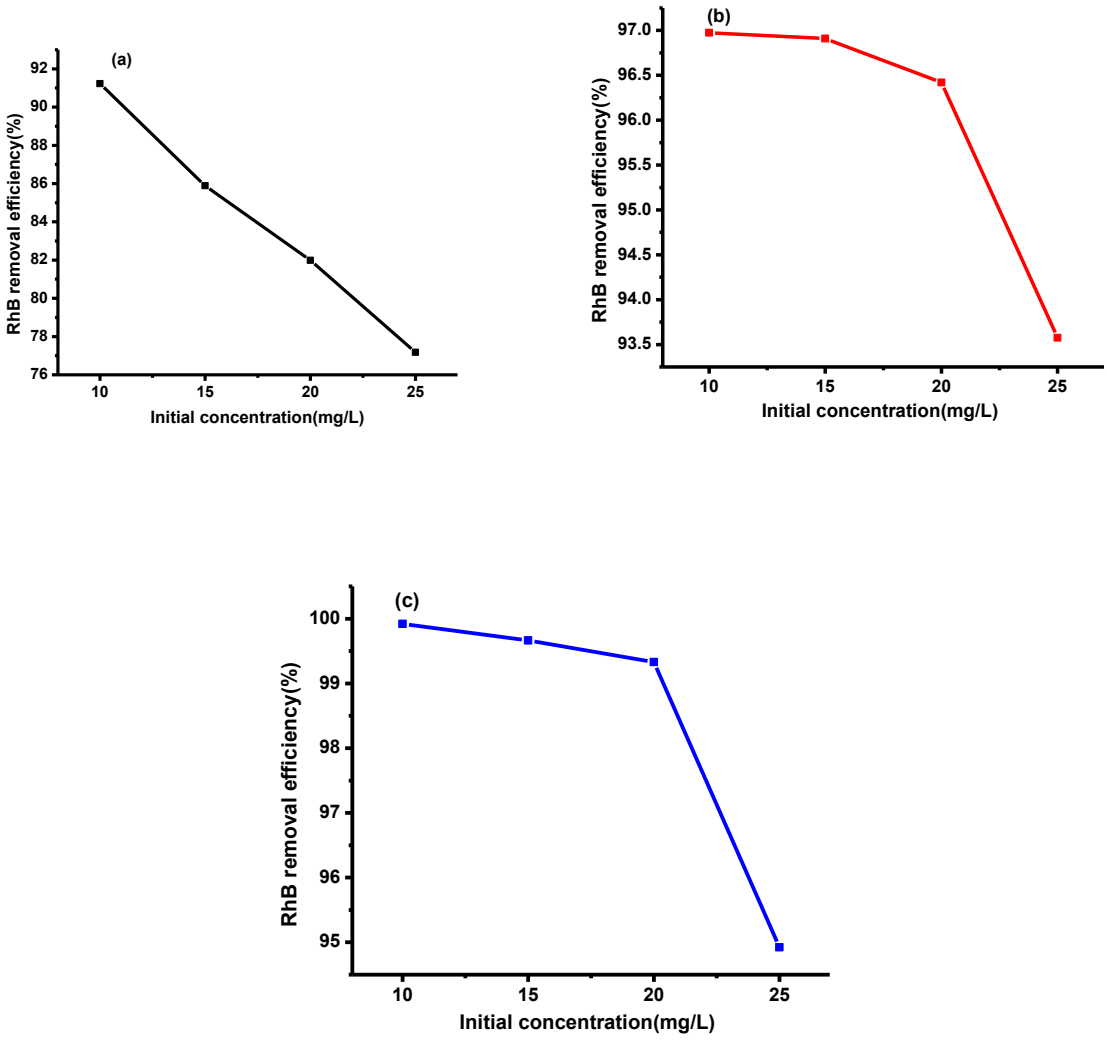

Figure 9: Effect of initial concentration on RhB dye removal by (a) PANI, (b) Fe3O4 NPs, and (c) PANI/ Fe3O4 adsorbent at pH 10, 80 mg adsorbent dose, 50 min contact time

4.5 Adsorption isotherm

When equilibrium is reached during adsorption, the adsorption isotherm shows how retained particles disperse between the liquid phase and the solid surface. Finding a suitable model requires first examining the isotherm data by fitting them to different isotherm models. Only the synthesized PANI, Fe_3O_4 NPs and PANI/Fe_3O_4 NPs adsorbent were included in the adsorption isotherm model. Freundlich and Langmuir adsorption isotherms were used to investigate the adsorbents.

4.5.1 Langmuir adsorption isotherm model

The creation of uniform monolayer coverage on the adsorbent surface, uniform adsorption energy, and the absence of molecular interaction between adsorbed molecules on nearby sites are the foundations of the Langmuir adsorption isotherm [103]. The concentration of dye in solution at equilibrium (Ce) and the amount of dye adsorbed per unit mass of adsorbent (q_e) can be used to study the adsorption isotherms. According to Md. Sandollah et al. (2020), the slope and the intercept of a linear form of the Langmuir equations were used to determine the Langmuir constant (K_L) and the maximum adsorption capacity (q_{max}).

$$\frac{Ce}{qe} = \frac{Ce}{q_{max}} + \frac{1}{q_{max}\, K_L} \quad \text{..... (Eq12)}$$

The values of q_{max} (mg/g) and K_L (L/mg) was determined from the plot of Ce vs Ce/qe. The adsorption capacity is often correlated with the variation in the area and porosity of the adsorbent. Higher surface area and pore volume resulted in higher adsorption capacity. The essential characteristics of the Langmuir isotherm model are often expressed by a dimensionless constant called the equilibrium parameter, R_L [104].

The maximum adsorption capacity (q_{max}), which denotes the saturated monolayer adsorption at equilibrium, was used to indicate Langmuir adsorption. PANI nanoparticles had Langmuir adsorption isotherm values of q_{max} (8.34 mg/g) and R^2 of 0.998, magnetite NPs had q_{max} (26.82 mg/g) and R^2 of 0.999, and the PANI/Fe_3O_4 NPs nanocomposite had q_{max} (745.84 mg/g) and R^2 of 0.999, according to the results displayed in Table 3. It shows that the nanocomposite q_{max} value and correlation coefficient (R^2) were superior to the surface area of a single precursor by rhodamine blue dye adsorption.

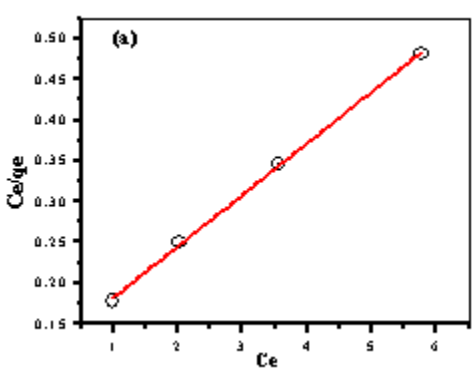

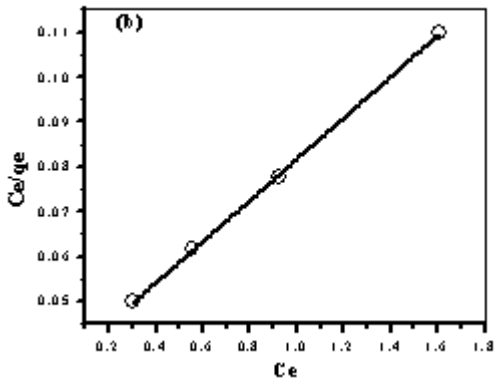

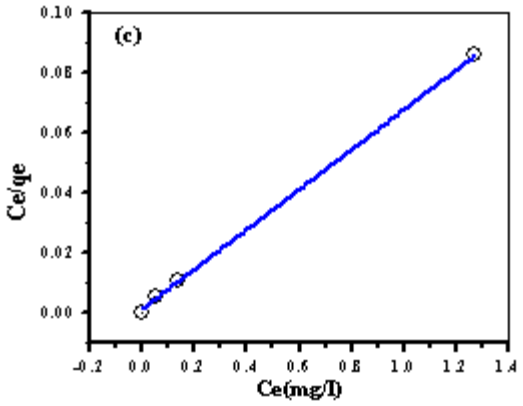

Figure 10: Langmuir adsorption isotherm model (a) for PANI, (b) for Fe3O4, and (c) for PANI/Fe3O4 adsorbent.

The Langmuir isotherm model provided the best linear fit for the adsorption investigation of RhB dye on PANI, Fe_3O_4, and PANI/Fe_3O_4 adsorbent, according to the correlation coefficient R^2 of Langmuir. For PANI, Fe_3O_4, and PANI/Fe_3O_4 adsorbent, the estimated values of the energy of adsorption constant (K_L) are 1.88 L/mg, 0.16 L/mg, and 0.01 L/mg, respectively. According to the Langmuir model, the R_L values calculated as 0.06, 0.14, and 0.80 were obtained between 0 and 1 for PANI, Fe_3O_4, and PANI/Fe_3O_4NPs nanocomposite, respectively.

Table 3: Parameters of Langmuir isotherm models for synthesized samples.

Langmuir isotherm model	synthesized samples		
	PANI	Fe_3O_4	PANI/Fe_3O_4 adsorbent
q_{max} (mg/g)	8.34	26.82	745.84
R_L	0.06	0.14	0.80
K_L (L/mg)	1.88	0.16	0.01
R^2	0.998	0.999	0.999

The Langmuir isotherm model is widely used to describe the adsorption behavior of solutes on adsorbent surfaces. It assumes that adsorption occurs on a surface with a finite number of identical sites and that once a site is occupied by a molecule, no further adsorption can occur at that site. The parameters of the Langmuir isotherm model—qmax, RL, KL, and R^2—provide important insights into the adsorption capacity and efficiency of the adsorbents.

Qmax represents the maximum adsorption capacity, indicating the maximum amount of dye (RhB in this case) that can be adsorbed per unit weight of the adsorbent. The results show that the PANI/Fe_3O_4 nanocomposite has the highest qmax value of 745.84 mg/g, which is significantly higher than Fe_3O_4 (26.82 mg/g) and PANI (8.34 mg/g). This suggests that the PANI/Fe_3O_4 nanocomposite has a far greater capacity to adsorb RhB dye, likely due to the synergistic effect between PANI and Fe_3O_4, which provides more active sites and enhances the overall adsorption.

For PANI, the RL value is 0.06, which indicates highly favorable adsorption, meaning the process is efficient. For Fe_3O_4, RL = 0.14 suggests favorable but less efficient adsorption than PANI. However, for the PANI/Fe_3O_4 nanocomposite, RL = 0.80 suggests a less favorable or moderately unfavorable adsorption, indicating that while the nanocomposite has a high adsorption capacity (as indicated by the high qmax), the adsorption process may be somewhat less efficient in comparison to pure PANI or Fe_3O_4 nanoparticles. This could be attributed to the potential

aggregation of Fe_3O_4 nanoparticles in the composite, which might reduce the accessibility of adsorption sites.

KL represents the affinity between the adsorbent and the adsorbate. A higher KL value suggests stronger adsorption, while a lower value indicates weaker adsorption. The PANI adsorbent has a high KL (1.88 L/mg), indicating a strong affinity between the PANI surface and RhB dye. In contrast, Fe_3O_4 (0.16 L/mg) and PANI/Fe_3O_4 adsorbent (0.01 L/mg) have much lower KL values, suggesting that their affinity for RhB dye is weaker than that of pure PANI. Despite the PANI/Fe_3O_4 nanocomposite having a lower KL value, its much higher qmax indicates that the composite's overall adsorption capacity is significantly better due to the synergistic effect between the components.

The R^2 value indicates the goodness of fit for the Langmuir isotherm model. An R^2 value close to 1 indicates a good fit, meaning the data closely follows the Langmuir adsorption isotherm. The high R^2 values of 0.998 for PANI, 0.999 for Fe_3O_4, and 0.999 for PANI/Fe_3O_4 nanocomposite suggest that the adsorption process for all three adsorbents closely follows the Langmuir model, confirming that the adsorption sites are homogeneous, and each dye molecule occupies only one site.

The PANI/Fe_3O_4 adsorbent shows superior adsorption capacity (qmax = 745.84 mg/g) compared to PANI (8.34 mg/g) and Fe_3O_4 (26.82 mg/g), despite having a less favorable RL (0.80) and lower KL (0.01 L/mg) values, which might indicate some level of reduced efficiency due to the composite structure. The PANI/Fe_3O_4 adsorbent is more effective in dye removal overall, likely due to its synergistic effect of combining the high adsorption capacity of PANI with the magnetic properties of Fe_3O_4. The high R^2 values for all adsorbents confirm that the adsorption of RhB dye is best described by the Langmuir isotherm, indicating that the adsorption process is monolayer and that the adsorption sites are uniform across the adsorbent surfaces. These findings suggest that PANI/Fe_3O_4 adsorbent is the most promising material for RhB dye removal, combining both high adsorption capacity and favorable isotherm characteristics.

4.5.2 Freundlich adsorption isotherm model

The Freundlich isotherm model is the earliest known relationship describing non-ideal and reversible adsorption, not restricted to the formation of a monolayer. This empirical model can be

applied to multilayer adsorption with a non-uniform distribution of adsorption heat and affinities over the heterogeneous surface [105]. The linear form of the Freundlich isotherm equation is as follows:

$$\ln qe = \ln Kf + \frac{1}{n} * \ln Ce \quad \text{..... (Eq13)}$$

Bond energies increase with surface density if 1/n = 1, decrease with surface density if 1/n > 1, and all surface sites are equivalent if 1/n = 1. The range of n values for favorable adsorption is 1–10, and a smaller value of the Freundlich equation coefficient 1/n indicates a better adsorption mechanism and the formation of a relatively stronger bond between adsorbate and absorbent [106].

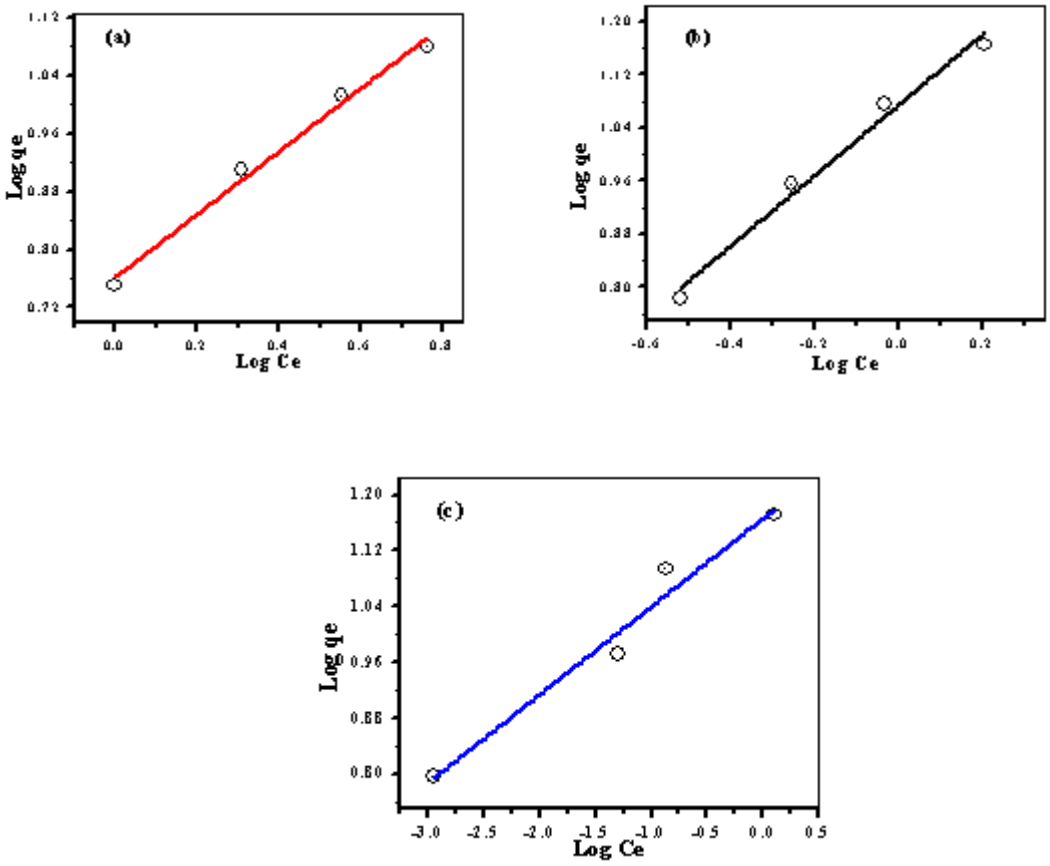

Figure 11: Freundlich adsorption isotherm models for (a) PANI, (b) Fe3O4, and (c) PANI/Fe3O4 adsorbent.

Since the Freundlich parameter of the 1/n value was between 0 and 1, the isotherm parameters result is shown in Table 4. This suggests that RhB dye adsorption on PANI, Fe_3O_4 NPs, and PANI/Fe_3O_4composite adsorbent is favorable. This implies that the binding between the RhB dye

and the three synthesized adsorbents was strong because the value of (n) is greater than 1. The adsorption process is beneficial in this work since the computed values of the Freundlich equation coefficient n (n = 2.24 for PANI, 2.04 for Fe_3O_4 NPs, and 6.58 for PANI/Fe_3O_4 NPs nanocomposite adsorbent) were more than 1.

NPs nanocomposite adsorbent has superior adsorption over PANI and magnetite NPs based on the Freundlich constant (K_F) values of PANI/Fe_3O_4. The reason for this is that the high K_F value indicates that the high adsorption PANI/Fe_3O_4 NPs NCs (13.40) is higher than that of Fe_3O_4 (10.68) and PANI (4.92). Furthermore, the PANI, Fe_3O_4, and PANI/Fe_3O_4 NPs nanocomposite adsorbents had Freundlich correlation coefficients of 0.982, 0.995, and 0.992, respectively. This suggests that among the three adsorbents, the Freundlich isotherm correlation coefficient R^2 was less than the Langmuir isotherm correlation coefficient. This suggests that for the three manufactured samples, the Langmuir isotherm model fits the rhodamine blue dye adsorption data better. The values of the constants and calculated parameters of the Freundlich isotherm are shown below in Table 4.

Table 4: Freundlich isotherm model parameters for synthesized samples

Freundlich isotherm model	synthesized samples		
	PANI	Fe_3O_4 NPs	PANI/Fe_3O_4 adsorbent
K_F (mg/g)	4.92	10.68	13.40
(n)	2.24	2.04	6.58
1/n	0.40	0.50	0.10
R^2	0.982	0.995	0.992

The Freundlich isotherm model is another widely used model for describing adsorption processes, particularly when adsorption occurs on heterogeneous surfaces with sites of varying energies. Unlike the Langmuir isotherm, the Freundlich model does not assume a monolayer adsorption, and it allows for multi-layer adsorption, which is common in systems with diverse adsorption sites.

The key parameters of the Freundlich isotherm model are KF, n, 1/n, and R^2, which provide insights into the adsorption capacity, intensity, and favorability of the adsorption process. Here, these parameters are presented for the three synthesized adsorbents:

The KF value indicates the adsorption capacity of the adsorbent. Higher KF values represent higher adsorption capacities. The PANI/Fe_3O_4 adsorbent has the highest KF value (13.40 mg/g), indicating that it has the highest adsorption capacity for RhB dye among the three adsorbents. This is consistent with the results from the Langmuir isotherm, where the nanocomposite showed the highest qmax value. Fe_3O_4 NPs and PANI have lower KF values of 10.68 mg/g and 4.92 mg/g, respectively, showing that they have lower dye adsorption capacities than the nanocomposite.

For PANI, Fe_3O_4 NPs, and PANI/Fe_3O_4 adsorbent, the n values are all greater than 1, indicating that the adsorption processes are favorable and that the adsorbents have a high degree of heterogeneity. However, PANI/Fe_3O_4 adsorbent has a significantly higher n value (6.58), which suggests a much higher level of heterogeneity compared to the other two adsorbents (PANI: 2.24 and Fe_3O_4: 2.04). This might indicate that the PANI/Fe_3O_4 nanocomposite provides a wider variety of adsorption sites, enhancing its overall adsorption capacity.

The 1/n value is often used as an indicator of the intensity of adsorption. A lower 1/n value suggests stronger adsorption at lower concentrations. In this case: PANI and Fe_3O_4 NPs have 1/n values of 0.40 and 0.50, respectively, indicating moderate adsorption intensity. PANI/Fe_3O_4 NPs nanocomposite has a much lower 1/n value (0.10), which indicates a higher adsorption intensity, meaning that the nanocomposite exhibits a more efficient adsorption process, particularly at lower concentrations of the dye.

For all three adsorbents, the R^2 values are quite high, suggesting that the adsorption of RhB dye onto PANI, Fe_3O_4 NPs, and PANI/Fe_3O_4 adsorbent are well described by the Freundlich isotherm. The Fe_3O_4 NPs and PANI/Fe_3O_4 NPs nanocomposite have exceptionally high R^2 values (0.995 and 0.992), indicating that their adsorption processes are very well represented by the Freundlich model, while PANI has a slightly lower R^2 value of 0.982, but still a strong fit.

The PANI/Fe_3O_4 NPs nanocomposite stands out as the most effective adsorbent based on KF (13.40 mg/g) and n (6.58) values, indicating both high adsorption capacity and greater heterogeneity compared to PANI and Fe_3O_4 NPs. The 1/n value of 0.10 further suggests that the

nanocomposite has a highly efficient adsorption mechanism, especially at lower concentrations of RhB dye.The Fe_3O_4 NPs and PANI also exhibit favorable adsorption characteristics but with lower adsorption capacities and less heterogeneity compared to the composite. The high R^2 values across all samples indicate that the Freundlich isotherm model is a good representation of the adsorption behavior, with the PANI/Fe_3O_4 NPs nanocomposite demonstrating the best overall performance in terms of both adsorption capacity and intensity. PANI/Fe_3O_4 NPs adsorbent are the most promising adsorbent for RhB dye removal, combining high adsorption capacity, favorable adsorption intensity, and high heterogeneity in the surface structure.

4.6 Adsorption kinetic studies

4.6.1 Pseudo-first order kinetics

The values of qe, k_1, K2, and R^2 are compiled in Table 5, and Figure 11, displays the linear curves plotted using pseudo-first-order and pseudo-second-order kinetics models. The pseudo-first-order kinetic model was used to study the kinetics of RhB adsorption onto PANI, Fe_3O_4 NPs, and PANI/Fe_3O_4 adsorbent. The conformity between experimental data of PANI was (4.85) and the calculated value (0.07), for Fe_3O_4 q_{exp} (5.12), q_{cal} (0.005), and for PANI/Fe_3O_4 NPs nanocomposite q_{exp} (5.88), q_{cal} (0.098) shows disagreement and also that the correlation coefficient R^2 was not close to unity, therefore it is not a favorable model for the adsorption of RhB onto the adsorbents as shown in Table 5, [107].

4.6.2 Pseudo-second order kinetics

As shown in Table 5, the calculated adsorption capacity from the pseudo-second-order model (4.80 mg/g) is closer to experimental data (4.85 mg/g) for PANI, q_{cal} (4.92 mg/g) is closer to q_{exp} (5.12 mg/g) for Fe_3O_4 NPs, and q_{cal} (5.42 mg/g) was closer to q_{exp} (5.88 mg/g) for PANI/Fe_3O_4 NPs nanocomposite adsorbent than that of the pseudo-first-order model. Additionally, the adsorption process of RhB from an aqueous solution matches the pseudo-second-order model better, as shown by the comparison of the two kinetics correlation coefficients (R^2). When comparing the pseudo-second-order kinetic model (0.999, 0.999, and 0.999) to the pseudo-first-order kinetic model (0.382, 0.344, and 0.356) for PANI, Fe_3O_4 NPs, and PANI/Fe_3O_4 adsorbent, respectively, the R^2 value approaches unity. The pseudo-second-order kinetic model that is produced, as seen in table 5, below, has a higher correlation coefficient value than the pseudo-first-order kinetic model, indicating that it more accurately fits the experimental adsorption data [109].

Table 5: Parameters of pseudo-1st order and pseudo-2nd order for synthesized samples

	PANI		Fe_3O_4 NPs		PANI/Fe_3O_4 adsorbent	
	Pseudo-1st order	Pseudo-2nd order	Pseudo-1st order	Pseudo 2nd-order	Pseudo - 1st order	Pseudo-2nd order
qe(experimental)	4.85	4.85	5.12	5.12	5.88	5.88
qe(calculated)	0.07	4.80	0.005	4.92	0.098	5.42
K	-0.00027	-0.248	0.00018	-0.412	-0.00083	-0.422
R^2	0.382	0.999	0.344	0.999	0.356	0.999

Pseudo-First-Order Kinetics: The pseudo-first-order model does not fit well for any of the synthesized adsorbents (PANI, Fe_3O_4 NPs, and PANI/Fe_3O_4 adsorbent) due to low R^2 values and poor agreement between the experimental and calculated qe values.

Pseudo-Second-Order Kinetics: The pseudo-second-order model provides a much better fit for the adsorption of RhB dye, with R^2 values of 0.999 for all three adsorbents. The calculated qe values for the pseudo-second-order model closely match the experimental qe values, especially for the PANI/Fe_3O_4 NPs adsorbent, which indicates that the adsorption process follows a second-order kinetic mechanism.

Adsorption Mechanism: The findings suggest that the PANI/Fe_3O_4 adsorbent exhibits the most effective adsorption behavior, aligning well with the pseudo-second-order model, which suggests that the adsorption is likely controlled by chemisorption, where the rate-limiting step involves chemical interactions between the RhB dye molecules and the adsorption sites on the nanocomposite.

The pseudo-second-order model is the most appropriate for describing the adsorption kinetics of RhB dye on the synthesized adsorbents, particularly the PANI/Fe_3O_4 adsorbent, which shows the best overall performance in terms of both adsorption capacity and kinetic behavior.

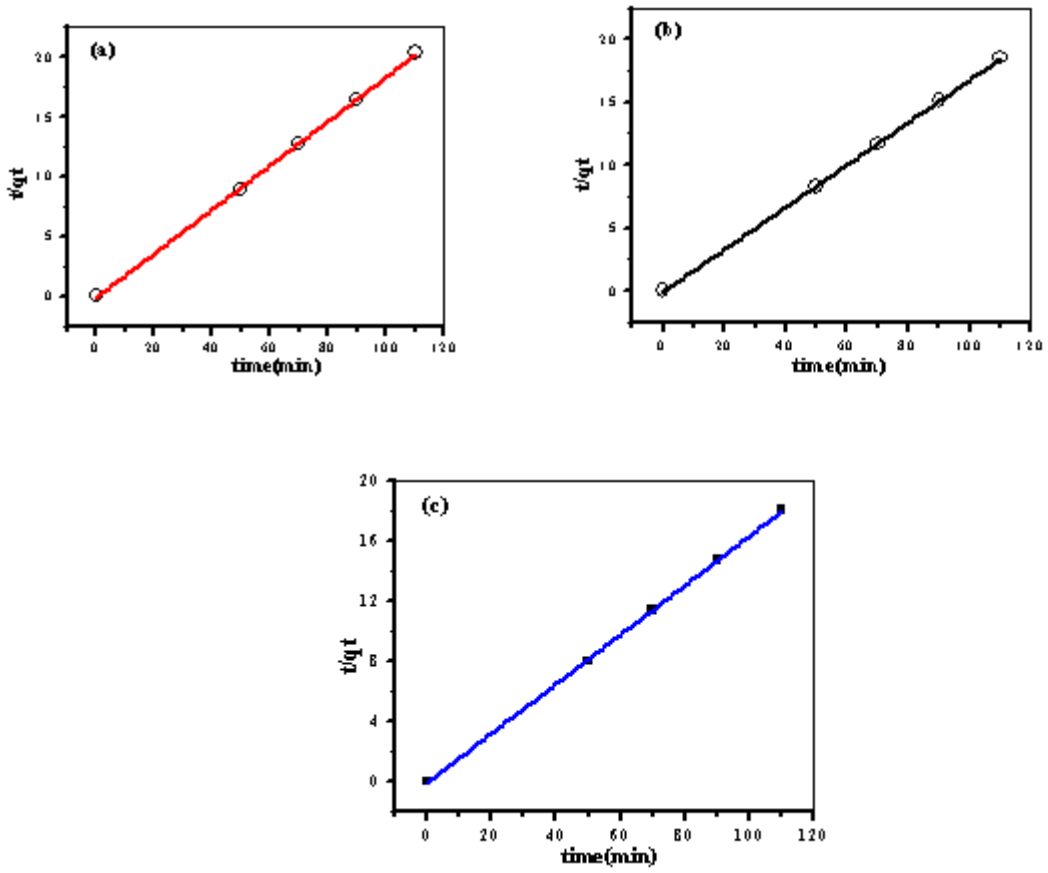

Figure 12: Pseudo second-order models of (a) PANI, (b) Fe3O4 NPs, and (c) PANI/Fe3O4adsorbent.

CHAPTER FIVE

5 CONCLUSION AND RECOMMENDATION

5.1 Conclusion

The present study presents a practical and environmentally friendly method for synthesizing PANI (polyaniline), Fe_3O_4 n, and their PANI/Fe_3O_4 adsorbent using an aqueous leave extract of *Croton macrostachyus.* The characterization of the synthesized adsorbent was conducted using a variety of techniques, including UV-DRS (Ultraviolet Diffuse Reflectance Spectroscopy), FTIR (Fourier Transform Infrared Spectroscopy). The UV-DRS analysis revealed the optical properties of the PANI, Fe_3O_4, and PANI/Fe_3O_4 adsorbent, while FTIR spectra confirmed the functional groups associated with the PANI polymer and Fe_3O_4 adsorbent as well as interactions between these components in the adsorbent. The XRD results indicated that the PANI/Fe_3O_4 adsorbent had an average particle size of 14 nm, which suggests that the PANI/Fe_3O_4 adsorbent has a fine, well-dispersed structure. In the adsorption experiments, the PANI/Fe_3O_4 adsorbent demonstrated the highest removal efficiency for Rhodamine B (RhB) dye from aqueous solutions, achieving a removal efficiency of 99.91%, significantly outperforming Fe_3O_4 NPs (96.97%) and PANI (91.22%). The adsorption capacity (qmax) of the PANI/Fe_3O_4 adsorbent was found to be 745.84 mg/g, far exceeding the adsorption capacities of Fe_3O_4 NPs (26.82 mg/g) and PANI (8.34 mg/g). These results indicate that the PANI/Fe_3O_4 adsorbent has a remarkable ability to adsorb large amount of dye. Several key factors that influence the efficiency of the adsorption process were investigated, including pH, adsorbent dosage, contact time, and initial concentration of RhB dye. The optimization of these parameters was critical in achieving the maximum dye removal efficiency. The adsorption isotherms were analyzed using the Langmuir and Freundlich models to understand the adsorption behavior of the synthesized adsorbents. The Langmuir isotherm model was found to fit the experimental data better than the Freundlich isotherm model. The maximum adsorption capacity (qmax) was higher for the PANI/Fe_3O_4 adsorbent, further confirming its superior adsorption capability. In terms of kinetics, the adsorption data were best described by the pseudo-second-order model. Given their high adsorption capacities, ease of synthesis, and strong interaction with dye molecules, PANI/Fe_3O_4 adsorbent hold great promise for widespread use in wastewater treatment, particularly in the removal of hazardous dyes from industrial effluents.

5.2 Recommendation

Based on the findings from the current research, a promising green synthesis approach involving cinnamon bark aqueous extract could be employed to prepare PANI/Fe_3O_4 adsorbent, which have demonstrated potential as effective adsorbents for removing Rhodamine Blue (RhB) dye from aqueous solutions. To further understand the structure, composition, and performance of the PANI/Fe_3O_4 adsorbent, additional characterization techniques would provide more detailed and comprehensive information about its properties. Energy-Dispersive X-ray Spectroscopy (EDX): EDX analysis would be crucial for assessing the elemental composition of the PANI/Fe_3O_4 adsorbent. Scanning Electron Microscopy (SEM): SEM would be useful for investigating the surface morphology of adsorbent. This technique provides high-resolution images of the surface, revealing particle size, shape, and surface text. Transmission Electron Microscopy (TEM): To obtain more specific and detailed information on the nanoscale structure of the adsorbent. TEM can provide high-resolution images that show the internal structure of the adsorbent at atomic and nonmetric scales. Bruner-Emmett-Teller (BET) Surface Area Analysis: A BET surface area analysis would be another important characterization tool to assess the porosity and surface area of the PANI/Fe_3O_4 adsorbent. This method helps determine the specific surface area, which is crucial in understanding the adsorption potential of the adsorbent. These characterization techniques, when used in combination, will provide a holistic understanding of the PANI/Fe_3O_4 adsorbent properties, such as its structure, chemical composition, morphology, and adsorption capacity. Further studies incorporating these methods could lead to a deeper understanding of the mechanisms of dye removal and adsorption dynamics, optimizing the material for real-world applications in wastewater treatment. By examining these advanced properties, future research can explore not only the efficiency of the adsorbent but also its reusability and long-term stability under various environmental conditions. This will provide valuable insights into the practicality of using green-synthesized PANI/Fe_3O_4 adsorbent as sustainable and efficient adsorbents for water purification and the removal of toxic pollutants from industrial wastewater.

6 REFERENCES

1. Ali Othman, E. D. (2018). Nano porous sorbents for the removal and recovery of phosphorus from eutrophic waters: sustainability challenges and solutions. ACS Sustainable Chem. Eng., 1-20.
2. Kartika, T., &Rathinamoorthy, R. (2015). Recycling and reuse of textile effluent sludge. *Environmental Implications of Recycling and Recycled Products*, 213-258.
3. S. Eftekhari, A. Habibi-Yangjeh, Sh. Sohrabnezhad, Application of AlMCM-41 for competitive adsorption of methylene blue and rhodamine B: thermodynamic and kinetic studies, J. Hazard. Mater. 178 (2010) 349–355.
4. J.M. Montaged, A. Duran, C. López-Almodóvar, Homogenous ferrioxalateassisted solar photo-Fenton degradation of orange II aqueous solutions, Appl. Cattel. B: Environ. 83 (2008) 46–55.
5. C. Marc, S. Marc, M.M. Joachim, G. Ingmar, Degradation of reactive dyes in wastewater from the textile industry by ozone: analysis of the products by accurate masses, Water Res. 43 (2009) 733–743.
6. A.B. dos Santos, F.J. Cervantes, J.B. van Lier, Review paper on current technologies for depolarization of textile wastewaters: perspectives for anaerobic biotechnology, Bio resource Technol. 98 (2007) 2369–2385.
7. Y. El Mouzdahir, A. Elmchaouri, R. Mahboub, A. Gil, S.A. Korili, Adsorption of methylene blue from aqueous solutions on a Moroccan clay, J. Chem. Eng. Data 52 (2007) 1621–1625.
8. T. Aarthi, P. Narahari, G. Madras, Photo catalytic degradation of Azure and Sudan dyes using nano TiO2, J. Hazard. Mater. 149 (2007) 725–734
9. Mamun Reshid, N.T. (2017). Effective removal of phosphate from aqueous solution using humic acid coated magnetite nanoparticles. Water research 123 (2017), 353-360.
10. Gospodinova, N., &Terlemezyan, L. (1998). Conducting polymers prepared by oxidative polymerization: polyaniline. *Progress in polymer science*, *23*(8), 1443-1484.
11. Amen, S., Akhtar, M. S., Song, M., & Shin, H. S. (2013). Metal oxide nanomaterials, conducting polymers and their nanocomposites for solar energy. *Solar Cells-Research and Application Perspectives*, 203-259.
12. Yeamin, B. (2012). Preparation of nano-materials and their recyclable application in the removal of organic dyes from aqueous solution.

13. Takai, Z. I., Mustafa, M. K., & Asman, S. (2018). Preparation of high performance conductive polyaniline magnetite (PANI/Fe3O4) Nanocomposites by Sol-Gel Method. *Asian J. Chem*, *30*(12), 2625-2630.
14. Meresa, A. (2019). Ethno medicinal uses, photochemistry and anti-malarial effect of Croton macrostachyus (Bisana): A review. *Journal of Medicinal Plants*, *7*(2), 79-88. Bashir I, Lone FA, Bhat RA, Mir SA, Dar ZA, Dar SA. Concerns and threats of contamination on aquatic ecosystems. Bioremediation bioethanol 2020; 27:1-26. DOI: https://doi.org/10.1007/978-3-030-35691-0_1
15. Wang, H., Yuan, X., Zeng, G., Lang, L., Peng, X., Liao, K., Peng, L., & Xiao, Z. (2014). Removal of malachite green dye from wastewater by different organic acid-modified natural adsorbent: Kinetics, equilibriums, mechanisms, practical application, and disposal of dye-loaded adsorbent. *Environmental Science and Pollution Research*, *21*(19), 11552–11564. https://doi.org/10.1007/s11356-014-3025-2
16. Siddiqua A, Hahladakis JN, Al-Attiya WAKA. An overview of the environmental pollution and health effects associated with waste landfilling and open dumping. Environ Sic Pollut Res Into 2022;
17. Ingra C, Strippable R, Lagidis G, Huisingh D. Water scarcity in agriculture: An overview of causes, I'm-pacts and approaches for reducing the risks. Helicon 2023; 9(8):e18507. DOI: https://doi.org/10.1016/j.heliyon.2023.e18507
18. Webster.com. (2010). Definition from Webster Dictionary 08-13 Retrieved 2010-08-26 Wikipedia, the free encyclopedia.http://en.wikipedia.or/wiki/pollution. Retrieved 20-06-2013.
19. G. Abate, J.C. Masini, Adsorption of atrazine, hydroxyatrazine, deethylatrazine, and deisopropylatrazine onto Fe(III) polyhydroxy cations intercalated vermiculite and montmorillonite, J. Agric. Food Chem. 53 (2005) 1612– 1619
20. Kuppusamy, S., Sethurajan, M., Kadarkarai, M., &Aruliah, R. (2017). Biodecolourization of textile dyes by novel, indigenous Pseudomonas stutzeri MN1 and Acinetobacter baumannii MN3. *Journal of environmental chemical engineering*, *5*(1), 716-724.
21. Earth, P., & Switzerland, G. C. (2016). World's worst pollution problems. *The new top six toxic threats: A priority list for remediation*.

22. Vickers, N. J. (2017). Animal communication: when I'm calling you, will you answer too? *Current biology*, *27*(14), R713-R715.
23. Abid, M. F., Zablouk, M. A., & Abid-Alameer, A. M. (2012). Experimental study of dye removal from industrial wastewater by membrane technologies of reverse osmosis and nanofiltration. *Iranian journal of environmental health science & engineering*, *9*, 1-9.
24. Dil, E. A., Ghaedi, M., Ghezelbash, G. R., &Asfaram, A. (2017). Multi-responses optimization of simultaneous bio sorption of cationic dyes by live yeast Yarrowialipolytica 70562 from binary solution: application of first order derivative spectrophotometry. *Ecotoxicology and environmental safety*, *139*, 158-164.
25. Melo, R. P. F., de Barros Neto, E. L., Moura, M. C. P. D. A., de Castro Dantas, T. N., Dantas Neto, A. A., & Nunes, S. K. D. S. (2017). Removal of Direct Yellow 27 dye by ionic flocculation: the use of an environmentally friendly surfactant. *Journal of Surfactants and Detergents*, *20*(2), 459-465.
26. Manavi, N., Kazemi, A. S., &Bonakdarpour, B. (2017). The development of aerobic granules from conventional activated sludge under anaerobic-aerobic cycles and their adaptation for treatment of dyeing wastewater. *Chemical Engineering Journal*, *312*, 375-384.
27. Rajasimman, M., Babu, S. V., & Rajamohan, N. (2017). Biodegradation of textile dyeing industry wastewater using modified anaerobic sequential batch reactor–Start-up, parameter optimization and performance analysis. *Journal of the Taiwan Institute of Chemical Engineers*, *72*, 171-181.
28. Asfaram, A., Ghaedi, M., Ghezelbash, G. R., & Pepe, F. (2017). Application of experimental design and derivative spectrophotometry methods in optimization and analysis of bio sorption of binary mixtures of basic dyes from aqueous solutions. *Ecotoxicology and environmental safety*, *139*, 219-227.
29. Kokunešoski, M., Gulicovski, J., Matović, B., Logar, M., Milonjić, S. K., & Babić, B. (2010). Synthesis and surface characterization of ordered mesoporous silica SBA-15. *Materials Chemistry and Physics*, *124*(2-3), 1248-1252.
30. Issa, A. A., Abdel-Halim, H. M., Al-Degs, Y. S., & Al-Masri, H. A. (2017). Application of multivariate calibration for studying competitive adsorption of two problematic colorants on acid-activated-kaolinitic clay. *Research on Chemical Intermediates*, *43*, 523-544.

31. Khosravi, M., & Azizian, S. (2014). Adsorption of anionic dyes from aqueous solution by iron oxide nanospheres. *Journal of Industrial and Engineering Chemistry*, *20*(4), 2561-2567.
32. Li, N., & Lei, X. M. (2012). Adsorption of ponceau 4R from aqueous solutions by polyamidoamine–cyclodextrin crosslinked copolymer. *Journal of Inclusion Phenomena and Macrocyclic Chemistry*, *74*, 167-176.
33. Wang, D., Liu, L., Jiang, X., Yu, J., & Chen, X. (2015). Adsorption and removal of malachite green from aqueous solution using magnetic β-cyclodextrin-graphene oxide nanocomposites as adsorbents. *Colloids and Surfaces A: Physicochemical and Engineering Aspects*, *466*, 166-173.
34. Zhang, Y., Huang, G., an, C., Xin, X., Liu, X., Raman, M. ... & Doble, M. (2017). Transport of anionic azo dyes from aqueous solution to Gemini surfactant-modified wheat bran: synchrotron infrared, molecular interaction and adsorption studies. *Science of the Total Environment*, *595*, 723-732.
35. Namvari, M., & Namazi, H. (2016). Magnetic sweet graphene nanosheets: preparation, characterization and application in removal of methylene blue. *International journal of environmental science and technology*, *13*, 599-606.
36. Moawed, E. A., El-Hagrasy, M. A., & Farhat, A. A. (2017). Application of magnetic isothiouronium polyurethane sorbent for the removal of acidic and basic dyes from wastewater. *Journal of Cleaner Production*, *157*, 232-242.
37. Buntić, A. V., Pavlović, M. D., Antonović, D. G., Šiler-Marinković, S. S., & Dimitrijević-Branković, S. I. (2017). A treatment of wastewater containing basic dyes by the use of new strain Streptomyces microflavus CKS6. *Journal of cleaner production*, *148*, 347-354.
38. Rybczyńska-Tkaczyk, K., &Korniłłowicz-Kowalska, T. (2016). Biosorption optimization and equilibrium isotherm of industrial dye compounds in novel strains of microscopic fungi. *International Journal of Environmental Science and Technology*, *13*, 2837-2846.
39. Deniz, F., &Ersanli, E. T. (2016). Removal of colorant from simulated wastewater by phono-composite material: Equilibrium, kinetic and mechanism studies in a lab-scale application. *Journal of Molecular Liquids*, *220*, 120-128.

40. Piaskowski, K., Świderska-Dąbrowska, R., & Zarzycki, P. K. (2018). Dye removal from water and wastewater using various physical, chemical, and biological processes. *Journal of AOAC International*, *101*(5), 1371-1384.
41. Zarzycki, P. K., Fenert, B., Kaleniecka, A., & Zarzycka, M. B. (2017). Hopanoids in cyanobacteria biomass and related samples. *Studies in Natural Products Chemistry*, *54*, 87-107.
42. Yahia, I.S., Rammah, Y.S., Khaled, K.F., 2013. Fabrication of an electrochemical cell based on Rhodamine B Dye for low power applications. J. Mater. Environ. Sci. 4 (3), 442–447.
43. Liu, K., Li, H., Wang, Y., Gou, X., Duan, Y., 2015. Adsorption and removal of rhodamine B from aqueous solution by tannic acid functionalized graphene. Colloid. Surface. Physicochemical. Eng. Aspect. 477, 35–41.
44. Chauhan, V.M., Hopper, R.H., Ali, S.Z., King, E.M., Urea, F., Oxley, C.H., Allot, J.W., 2014. Thermo-optical characterization of fluorescent rhodamine B based temperature-sensitive nanosensors using a CMOS MEMS micro-hotplate. Sensor. Actuator. B Chem. 192, 126–133
45. Singh, S., Kumar, A., Gupta, H., 2020. Activated banana peel carbon: a potential adsorbent for Rhodamine B decontamination from aqueous system. Applied Water Science 10 (8), 1–8.
46. Manzoor, J., Sharma, M., 2020. Impact of textile dyes on human health and environment. In: Impact of Textile Dyes on Public Health and the Environment. IGI Global, pp. 162–169
47. Foo, K.Y., Hameed, B.H., 2010. Decontamination of textile wastewater via TiO2/ activated carbon composite materials. Adv. Colloid Interface Sci. 159 (2), 130–143
48. Imran, M., Crowley, D.E., Khalid, A., Hussain, S., Mumtaz, M.W., Arshad, M., 2015. Microbial biotechnology for decolourization of textile wastewaters. Rev. Environ. Sci. Biotechnology. 14 (1), 73–92.
49. Hassan, H.F., Hassan, U.F., Usher, O.A., Ibrahim, A.B., Table, N.N., 2018. Exploring the potentials of Banana (Musa Sputum) peels in feed formulation. Int. J. Adv. Res. Compute. Sci. 5, 10–14.

50. E.N. Zare, A. Motahari, M. Sillanpa ¨¨ a, Nanoadsorbents based on conducting polymer nanocomposites with main focus on polyaniline and its derivatives for removal of heavy metal ions/dyes: A review, Environmental Research 162 (2018) 173–195.
51. A. Muhammad, A.-u.-H.A. Shah, S. Bilal, G. Rahman, Basic Blue Dye Adsorption from Water using Polyaniline/Magnetite (Fe3O4) Composites: Kinetic and Thermodynamic Aspects, Materials 12 (2019) 1764
52. A. Nasar, F. Mashkoor, Application of polyaniline-based adsorbents for dye removal from water and wastewater—a review, Environmental Science and Pollution Research 26 (2019) 5333–5356.
53. S. Mondal, U. Rana, P. Das, S. Malik, Network of Polyaniline Nanotubes for Wastewater Treatment and Oil/Water Separation, ACS Applied Polymer Materials 1 (2019) 1624–1633.
54. T.L.A. Campos, D.F. Kersting, C.A. Ferreira, Chemical synthesis of polyaniline using sulphanilic acid as dopant agent into the reactional medium, Surface and Coatings Technology 122 (1999) 3–5.
55. X.-X. Liu, L. Zhang, Y.-B. Li, L.-J. Bian, Z. Su, L.-J. Zhang, Electro polymerization of aniline in aqueous solutions at pH 2 to 12, Journal of materials science 40 (2005) 4511–4515
56. J. Wang, L. Bi, Y. Jib, H. Ma, X. Yin, Removal of humic acid from aqueous solution by magnetically separable polyaniline: Adsorption behavior and mechanism, Journal of Colloid and Interface Science 430 (2014) 140–146.
57. T.C. Maponya, M.J. Hato, T.R. Somo, K.E. Ramohlola, M.D. Mokhafola, G. R. Monama, A. Maity, K.D. Modibane, L.M. Katata-Seru, Polyaniline-Based Nanocomposites for Environmental Remediation, in, Heavy Metal Ions Removal, IntechOpen (2019)
58. Y. Zheng, W. Wang, D. Huang, A. Wang, Kapok fber oriented-polyaniline nanofbers for effcient Cr (VI) removal, Chemical Engineering Journal 191 (2012) 154–161.

59. Y. Liu, L. Song, L. Du, P. Gao, N. Liang, S. Wu, T. Minami, L. Zang, C. Yu, X. Xu, Preparation of Polyaniline/Emulsion Microsphere Composite for Effcient Adsorption of Organic Dyes, Polymers (Basel) 12 (2020) 167.
60. Y. Jiang, Z. Liu, G. Zeng, Y. Liu, B. Shao, Z. Li, Y. Liu, W. Zhang, Q. He, Polyaniline-based adsorbents for removal of hexavalent chromium from aqueous solution: a mini review, Environ Sic Pollut Res 25 (2018) 6158–6174.
61. X. Jiang, J. Cheng, H. Zhou, F. Li, W. Wu, K. Ding, Polyaniline-coated chitosan functionalized magnetic nanoparticles: Preparation for the extraction and analysis of endocrine-disrupting phenols in environmental water and juice samples, Talent 141 (2015) 239–246.
62. R. Ahmad, I. Hasan, A. Mittal, Adsorption of Cr (VI) and Cd (II) on chitosan grafted polyaniline-OMMT nanocomposite: isotherms, kinetics and thermodynamics studies, Desalin Water Treat 58 (2017) 144–153
63. X. Liu, B. Wang, G. Jing, Y. Qian, Kinetics, isotherms, and mechanism of Cr (VI) adsorption by polyaniline/sunflower stem pith composite adsorbent, desalination and water treatment 141 (2019) 197–207.
64. M.S. Alshammari, A.A. Essay, A. El-Nggar, S. Sayyah, Ultrasonic-Assisted Synthesis and Characterization of Chitosan-Graft-Substituted Polyanilines: Promise Bio-Based Nanoparticles for Dye Removal and Bacterial Disinfection, Journal of Chemistry 2020 (2020).
65. Ali, A., Zafar, H., Zia, M., Ul Haq, I., Phull, A. R., Ali, J. S., Hussain, A. (2016). Synthesis, characterization, applications, and challenges of iron oxide nanoparticles. *Nanotechnology, Science and Applications, 9*, 49-67.
66. Ghazanfari, M. R., Kashefi, M., Shams, S. F., Jaafari, M. R. (2016). Perspective of Fe3O4 nanoparticles role in biomedical applications. *Biochemistry Research International, 2016*, 32.
67. R. M. Cornell, U. Schwertmann, *the Iron Oxides, Structure, Properties, Reactions, Occurr ences and Uses*, Wiley-VCH, 2nd Edition, 2003.
68. Jayanta Kumar, K.H. B. (2014). Green nanotechnology: Factors affecting synthesis and characterization technique. Hindawi publishing corporation, 1-13

69. Yen Pin Yew, K.S. (2018). Green biosynthesis of superparamagnetic magnetite nanoparticles and biomedical application in targeted anticancer drug delivery system: A review, Arabian journal of chemistry, 1-5.
70. K. Wakjira and L. Negash, "Germination responses of Croton macrostachyus (Euphorbiaceae) to various physico-chemical pretreatment conditions," South African Journal of Botany, vol. 87, pp. 76–83, 2013.
71. J. Dechasa, "Influence of Croton macrostachyus on maize yield: Traditional inter-crop farming system," Walia, vol. 1998, no. 20, p. pp, 1999
72. A. Maroyi, "Alternative medicines for HIV/AIDS in resourcepoor settings: Insight from traditional medicines use in subSaharan Africa," Tropical Journal of Pharmaceutical Research, vol. 13, no. 9, pp. 1527–1536, 2014.
73. T. Equal, G. Tuliahan, M. Gidey, and Y. Mekonnen, "In vitro anthelmintic activities of four Ethiopian medicinal plants against Haemonchuscontortus ,Pharmacologyonline," Pharmacologyonline, vol. 3, pp. 153–165, 2006
74. A. Amuamuta, Z. Mekonnen, and E. Gebeyehu, "Therapeutic usage and phytochemical screening study on some selected indigenous medicinal plants from Zegie and Lake Tana areas, Northwest Ethiopia," European Journal of Applied Sciences, vol. 6, no. 4, pp. 83–90, 2014.
75. Ravindra Kuman Gautam, M.C (2016). Nanotechnology for water cleanup. In M.C Ravindra Kumar Gautam, Nanomaterials for wastewater remediation (pp 10-12).
76. Imran Ali, C. P. (2019). Water purification using magnetic nanomaterials. In K. A. E Mohamed, magnetic nanostructure environmental and agricultural application, ram parasad (pp. 162-164). Switzerland springer nature publisher.
77. Sheshmani, S., & Mashhadi, S. (2018). Potential of magnetite reduced graphene oxide/chitosan nanocomposite as biosorbent for the removal of dyes from aqueous solutions. *Polymer Composites*, *39*, E457–E462. https://doi.org/10.1002/pc.24608
78. Ding, J., Pan, Y., Li, L., Liu, H., Zhang, Q., Gao, G., Pan, B., 2020. Synergetic adsorption and electrochemical classifed recycling of Cr(VI) and dyes in synthetic dyeing wastewater. Chem. Eng. J. 384, 123232 https://doi.org/10.1016/j.cej.2019.123232

79. Turkten, N., Karatas, Y., Bekbolet, M., 2021. Preparation of panimodifedzno composites via different methods: structural, morphological and photo catalytic properties. Water 13 (8), 1025. https://doi.org/10.3390/w13081025
80. Patil, M.R., Khairnar, S.D., Shrivastava, V.S., 2016. Synthesis, characterization of polyaniline–Fe3O4 magnetic nanocomposite and its application for removal of an acid violet 19 dye. Appl. Nonsocial. 6 (4), 495–502. https://doi.org/10.1007/s13204-015-0465-z.
81. DimitriesDermatas, T. M. (2018). Adsorption of ground water pollutants. In N. Q. Marta I. Litter, iron nanomaterials for water and soil treatment (pp. 41-43). Singapore pan Stanford publishing pts. Ltd.
82. Mengxue Li, J. L. (2016). Phosphate adsorption on metal oxides and metal hydroxides: A comparative review, environmenta review. 24, 319-332.
83. Namazi, M. P. (2020). Application of polysaccharide-based hydrogels for water treatments. In Y. chem, hydrogels based on natural polymers (pp. 411-444). Amsterdam, Netherlands: Elsevier publications.
84. Abate, G. Y., Alene, A. N., Habte, A. T., & Getahun, D. M. (2020). Adsorptive removal of malachite green dye from aqueous solution onto activated carbon of *Catha edulis* stem as a low cost bio-adsorbent. *Environmental Systems Research*, *9*(1). https://doi.org/10.1186/s40068-020-00191-4.
85. Moussout, H., Ahlafi, H., Aazza, M., &Maghat, H. (2018). ScienceDirect Critical of line rand nonlinear equations of pseudo-first order and pseudo-second order kinetic models.*Karbala International Journal of Modern Science*. https://doi.org/10.1016/j.kijoms.2018.04.001
86. Prasutiyo, Y. J., Manaf, A., & Hafizah, M. A. E. (2020). Synthesis of polyaniline by chemical oxidative polymerization and characteristic of conductivity and reflection for various strong acid dopants. In *Journal of Physics: Conference Series* (Vol. 1442, No. 1, p. 012003). IOP Publishing.
87. Rajput S., Pittman C. U., Mohan D., (2016), Magnetic magnetite (Fe_3O_4) nanoparticle synt hesis and applications for lead (Pb^{2+}) and chromium (Cr^{6+}) removal from water. *J. Colloid Interf. Sci*. 468: 334–346

88. IK, M., & 'Uthman ISAH, K. (2015). The effect on extracting solvents using natural dye extracts from hyphaenethebaica for dye-sensitized solar cells. *Journal of Material Science & Engineering*, *05*(01). https://doi.org/10.4172/2169-0022.1000208
89. Dandjesso, C. (2012). Photochemistry and hemostatic properties of some medicinal plants sold as anti-hemorrhagic in Cotonou Markets (Benin). *Indian Journal of Science and Technology*, *5*(8), 1–5. https://doi.org/10.17485/ijst/2012/v5i8.10
90. Mulushewa, Z., Dinbore, W. T., & Ayele, Y. (2021). Removal of methylene blue from textile waste water using kaolin and zeolite-x synthesized from Ethiopian kaolin. *Environmental Analysis Health and Toxicology*, *36*(1), e2021007. https://doi.org/10.5620/eaht.2021007.
91. Yuan, N., Cai, H., Liu, T., Huang, Q., & Zhang, X. (2019). Adsorptive removal of methylene blue from aqueous solution using coal fly ash-derived mesoporous silica material. *Adsorption Science & Technology*, *37*(3 to 4), 333 to 348. https://doi.org/10.1177/0263617419827438.
92. Masho, T. J., Arasu, P. T., Bogale, R. F., &Gendo, K. M. (2024). Green synthesis, characterization of Ag2O doped ZnO nanoparticles using aqueous extract of Croton macrostachyus leaf for photo degradation, and antioxidant activities. *Results in Chemistry*, *7*, 101478.
93. H. Zhang, X. Zhong, J.-J. Xu and H.-Y. Chen, *Langmuir*, **24**, 13748 (2008); https://doi.org/10.1021/la8028935.
94. W.J. Parka, T. Pellegrino and C. Plank, *Nanotechnology*, **16**, 9 (2005); https://doi.org/10.1088/0957-4484/16/2/R01.
95. P. Liu, W. Liu and Q. Xue, *Mater. Chem. Phys.*, **87**, 109 (2004); https://doi.org/10.1016/j.matchemphys.2004.05.001.
96. Barbaric M, Bal tog I, Lefrant S, Mevellec JY, Chauvet O (2003) Polyaniline and carbon nanotubes based composites containing whole units and fragments of nanotubes. Chem Mater 15:4149–4156. doi:10.1021/cm021287x
97. Gabal, R. A., Shokeir, D., & Orabi, A. (2022). *Cytotoxicity and Hemostatic One Step* Green *Synthesis of Iron Nanoparticles Coated with Green Tea for Biomedical Application*. *19*(3).
98. A.M. Granary, I. Jerkovic, V. Koncar, C. Cochrane, F.M. Kelly, D. Soulat and X. Legrand, *J. Ind. Text.*, **48**, 612 (2017); https://doi.org/10.1177/1528083717699368.

99. T.H. Hsieh, K.-S. Ho, X. Bi, Y.-K. Han, Z.-L. Chen, C.-H. Hsu and Y.-C. Chang, *Eur. Polyp. J.*, **45**, 613 (2009); https://doi.org/10.1016/j.eurpolymj.2008.12.039.
100. Das, S. K., Khan, M. M., Parandhaman, T., Lifar, F., Gotha, A. K., Sekaran, G., & Mandal, A. B. (2013). Nano-silica fabricated with silver nanoparticles: Antifouling adsorbent for efficient dye removal, effective water disinfection and biofouling control. *Nanoscale*, *5*(12), 5549. https://doi.org/10.1039/c3nr00856h
101. Wu, Q., Feng, C., Wang, C., & Wang, Z. (2013). A facile one-pot solvothermal method to produce superparamagnetic graphene–fe3o4 nanocomposite and its application in the removal of dye from aqueous solution. *Colloids and Surfaces B: Biointerfaces*, *101*, 210–214. https://doi.org/10.1016/j.colsurfb.2012.05.036
102. Elmorsi, T. M. (2011). Equilibrium isotherms and kinetic studies of removal of methylene blue dye by adsorption onto Miswak leaves as a natural adsorbent. *Journal of Environmental Protection*, *02*(06), 817 to 827. https://doi.org/10.4236/jep.2011.26093
103. Rahman, M. A., Amin, S. M., & Alam, A. M. (2012). Removal of methylene blue from waste water using activated carbon prepared from rice husk. *Dhaka University Journal of Science*, *60*(2), 185–189. https://doi.org/10.3329/dujs.v60i2.11491
104. Gamely, A. H., Elsharkawy, R. G., & Aboelfetoh, E. F. (2017). Graphene Oxide/Polyaniline/Manganese Oxide Ternary Nanocomposites, Facile Synthesis, Characterization, and Application for Indigo Carmine Removal. *Journal of Polymers and the Environment*, *26*(2), 655–669. https://doi.org/10.1007/s10924-017-0947-z.
105. Kavithad, D., & Namasivayam, C. (2007). Experimental and kinetic studies on methylene blue adsorption by Coir Pith Carbon. *Bio resource Technology*, *98*(1), 14–21. https://doi.org/10.1016/j.biortech.2005.12.008
106. Wang, H., Yuan, X., Zeng, G., Lang, L., Peng, X., Liao, K., Peng, L., & Xiao, Z. (2014). Removal of malachite green dye from wastewater by different organic acid-modified natural adsorbent: Kinetics, equilibriums, mechanisms, practical application, and disposal of dye-loaded adsorbent. *Environmental Science and Pollution Research*, *21*(19), 11552–11564. https://doi.org/10.1007/s11356-014-3025-2
107. Salsify, A. (2017). Fluoride removal from drinking water using granular aluminum-coated bauxite as adsorbent: Optimization of synthesis process conditions and equilibrium study.

Fluoride Removal from Groundwater by Adsorption Technology, 161–202. https://doi.org/10.1201/9781351199995-5

108. Hermawan, A. A., Bing, T. K., & Salamatinia, B. (2015). Application and optimization of using recycled pulp for methylene blue removal from wastewater: A response surface methodology approach. *International Journal of Environmental Science and Development*, *6*(4), 267–274. https://doi.org/10.7763/ijesd.2015.v6.602

109. Jazeera, P. K., Gervais's, J., & Joseph, A. (2019). Selective adsorption of methylene blue (MB) dye from aqueous mixture of MB and methyl orange (MO) using mesoporous titanic (tio2) – poly vinyl alcohol (PVA) nanocomposite. *Journal of Molecular Liquids*, *286*, 110908. https://doi.org/10.1016/j.molliq.2019.110908

110 Al-Saadi, A.A., Saleh, T.A., and Gupta, V.K., 2013, Spectroscopic and computational evaluation of cadmium adsorption using activated carbon produced from rubber tires, *J. Mol. Liq.*, 188, 136–142.

111 Nasrullah, A., Saad, B., Bhat, A.H., Khan, A.S., Danish, M., Isa, M.H., and Naeem, A., 2019, Mangos teen peel waste as a sustainable precursor for high surface area mesoporous activated carbon: Characterization and application for methylene blue

112 M. Loos, Allotropes of Carbon and Carbon Nanotubes, Carbon Nanotube Reinf. Compos. CNR Polym. Sci. Technol., 2015, 73–101, DOI: 10.1016/B978-1-4557-3195-4.00003-5.

113 B. Guo, Y. Zhao, W. Wu et al., "Research on the preparationtechnology of polyaniline nanofiber based on high gravitychemical oxidative polymerization," Chemical Engineeringand Processing Process Intensification, vol. 70, pp. 1–8, 2013.

114 da Rosa, A.L.D., Carissimi, E., Dotto, G.L., Sander, H., and Feris, L.A., 2018, Biosorption of Rhodamine B dye from dyeing stones effluents using the green microalgae *Chlorella pyrenoidosa*, *J. Cleaner Prod.*, 198, 1302–1310.

115Yoshimura, A.; Matsuno, Y. The improvement of platinum recovery ratio in the recycling process using "dry aqua regain". Mater.Trans. **2019**, 60, 2223–2228. [CrossRef]

116.Youssef, A.M. Recovery and then individual separation of platinum, palladium, and rhodium from spent car catalytic converters using hydrometallurgical technique followed by successive precipitation methods. J. Chem. **2019**, 2019, 2318157. [CrossRef]

117.Xing, W.D.; Lee, M.S. A process for the separation of noble metals from HCL liquor containing gold(III), palladium(II), platinum(IV), rhodium(III), and iridium(IV) by solvent extraction. Processes **2019**, 7, 18–20.

118.Nguyen, T.H.; Lee, M.S. Effect of HCl concentration on the oxidation of LIX 63 and the subsequent separation of Pd(II), Pt(IV),Ir (IV) and Rh(III) by solvent extraction. J. Korean Inst. Met. Mater. **2016**, 54, 768–774.

119.Yamani, J. S., Lounsbury, A. W., & Zimmerman, J. B. (2014). Adsorption of selenite and selenite by nanocrystalline aluminum oxide, neat and impregnated in chitosan beads. *Water research*, *50*, 373-381.

120.Yang, J., Hour, B., Wang, J., Tina, B., Bi, J., Wang, N., & Huang, X. (2019). Nanomaterial for the removal of heavy metals from wastewater. *Nanomaterial*, *9*(3), 424.

121.Wang, X., Zhan, C., Kong, B., Zhu, X., Liu, J., Xu, W ., & Wang, H. (2015). Self-curled coral-like γ-Al2O3 nanoplates for use as an adsorbent. *Journal of colloid and interface science*, *453*, 244-251.

122.R. D.Monte, J.Kaspar; Catal.Today100 (2005)27.

123.M. Arias, C. Novo, E. Lopez and B. Soto, Georama, 133 (2006) 151-159.

124 Yu, Y.; Murthy, B.N.; Shapter, J.; Constantopoulos, K.T.; Voelcker, N.; Ellis, A. Benzene carboxylic acid derivatized graphene oxidenanosheets on natural zeolites as effective adsorbents for cationic dye removal. J. Hazard. Mater. **2013**, 260, 330–338. [CrossRef]

7Appendix

Figure1: weighing of powdered plant

Figure 2: plant extract

Figure 3: Synthesis of nanoparticles

Figure 4: weight balance of adsorbent

Figure 5: picture of pH adjustment in optimization